USGS
science for a changing world

Hydrogeologic Investigations of the Miocene Nogales Formation in the Nogales Area, Upper Santa Cruz Basin, Arizona

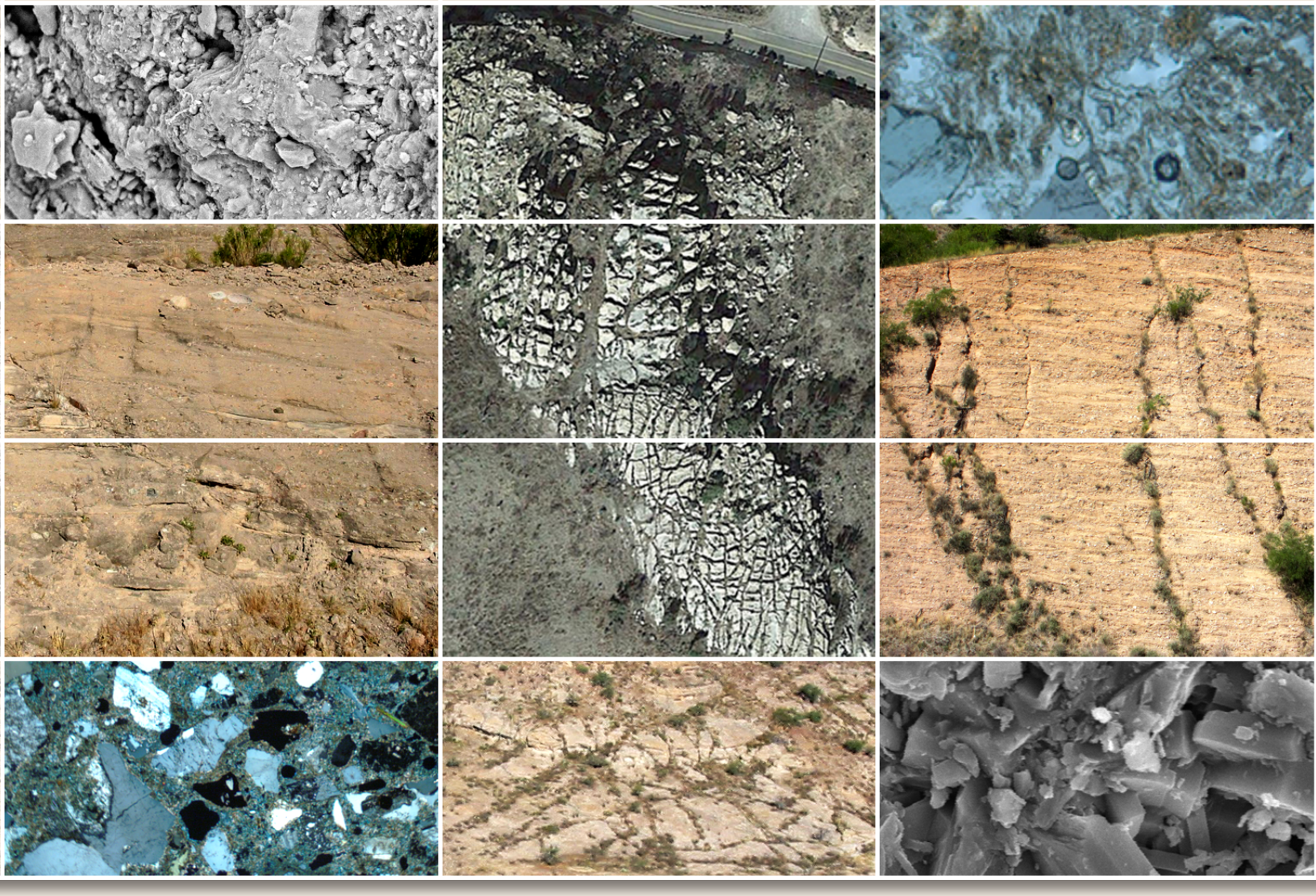

Scientific Investigations Report 2016–5087

U.S. Department of the Interior
U.S. Geological Survey

Hydrogeologic Investigations of the Miocene Nogales Formation in the Nogales Area, Upper Santa Cruz Basin, Arizona

By William R. Page, Floyd Gray, Mark W. Bultman, and Christopher M. Menges

Scientific Investigations Report 2016–5087

U.S. Department of the Interior
U.S. Geological Survey

U.S. Department of the Interior
SALLY JEWELL, Secretary

U.S. Geological Survey
Suzette M. Kimball, Director

U.S. Geological Survey, Reston, Virginia: 2016

For more information on the USGS—the Federal source for science about the Earth, its natural and living resources, natural hazards, and the environment—visit http://www.usgs.gov or call 1–888–ASK–USGS.

For an overview of USGS information products, including maps, imagery, and publications, visit http://store.usgs.gov.

Any use of trade, firm, or product names is for descriptive purposes only and does not imply endorsement by the U.S. Government.

Although this information product, for the most part, is in the public domain, it also may contain copyrighted materials as noted in the text. Permission to reproduce copyrighted items must be secured from the copyright owner.

Suggested citation:
Page, W.R., Gray, Floyd, Bultman, M.W., and Menges, C.M., 2016, Hydrogeologic investigations of the Miocene Nogales Formation in the Nogales area, upper Santa Cruz basin, Arizona: U.S. Geological Survey Scientific Investigations Report 2016–5087, 31 p., http://dx.doi.org/10.3133/sir20165087.

ISSN 2328-0328 (online)

Contents

Figures

All photographs taken by the author unless otherwise noted.

Appendix Figure

Tables

Conversion Factors

U.S. customary units to International System of Units

Multiply	By	To obtain
	Length	
foot (ft)	30.48	centimeter (cm)

International System of Units to U.S. customary units

Multiply	By	To obtain
	Length	
centimeter (cm)	0.3937	inch (in.)
meter (m)	3.281	foot (ft)
meter (m)	1.094	yard (yd)
kilometer (km)	0.6214	mile (mi)
	Density	
gram per cubic centimeter (g/cm^3)	62.4220	pound per cubic foot (lb/ft^3)

Temperature in degrees Celsius (°C) may be converted to degrees Fahrenheit (°F) as °F = (1.8 × °C) + 32.

Abbreviations

SEM scanning electron microscope

SHC saturated hydraulic conductivity

XRD x-ray diffraction

cm/d centimeter per day

cm/s centimeter per second

ft/d foot per day

g/cm^3 gram per cubic centimeter

km kilometer

m meter

Ma mega-annum (million years ago)

µm micrometer

Hydrogeologic Investigations of the Miocene Nogales Formation in the Nogales Area, Upper Santa Cruz Basin, Arizona

By William R. Page, Floyd Gray, Mark W. Bultman, and Christopher M. Menges

Abstract

Hydrogeologic investigations were conducted to evaluate the groundwater resource potential for the Miocene Nogales Formation in the Nogales area, southern Arizona. Results indicate that parts of the formation may provide new, deeper sources of groundwater for the area. Geologic mapping determined the hydrogeologic framework of the formation by defining lithologic, mineralogic, and stratigraphic characteristics; identifying potential aquifers and confining units; and mapping faults and fractures which likely influence groundwater flow. Geophysical modeling was used to determine the basin geometry and thickness of the Nogales Formation and younger alluvial aquifers and to identify target areas (deep subbasins) which may prove to be productive aquifers.

Volcaniclastic sandstone samples from the formation were analyzed for porosity, bulk density, saturated hydraulic conductivity, and fabric. Effective porosity ranges from 16 to 42 percent, bulk density from 1.6 to 2.47 grams per cubic centimeter, and saturated hydraulic conductivity (SHC) from 4 to 57 centimeters per day (4.9×10^{-5} to 6.7×10^{-4} centimeters per second). Thin sections show that sandstone framework grains consist of quartz, feldspar, biotite, hornblende, pumice, volcanic glass, and opaque minerals. The matrix in most samples consists of pumice fragments, and some contain predominantly silt and clay. Samples with a mostly silt and clay matrix have lower porosity and SHC compared to samples with mostly pumice, which have higher and wider ranges of porosity and SHC. Pore space in the Nogales Formation sediments includes moldic, intercrystalline, and fracture porosity. Some intercrystalline pore space is partially filled with calcite cement. About one third of the samples contain fractures, which correspond to fractures noted in outcrops in all members of the formation.

Scanning electron microscope (SEM) and x-ray diffraction (XRD) analyses indicate that most of the samples contained the zeolite clinoptilolite and mixed-layer clay. X-ray diffraction analyses verified clinoptilolite as the only zeolite in Nogales Formation samples; they also verified the presence of smectite and illite clay and some kaolinite. Samples which contain greater amounts of clinoptilolite and lesser amounts of smectite have high porosity and SHC in narrow ranges. However, samples with abundant smectite and lesser amounts of clinoptilolite span the entire ranges of porosity and SHC for the formation.

All members of the Nogales Formation are fractured and faulted as a result of Tertiary Basin and Range extensional deformation, which was broadly contemporaneous with deposition of the formation. These structures may have significant influence on groundwater flow in the upper Santa Cruz basin because, although many of the sediments in the formation have characteristics indicating they may be productive aquifers based only on porous-media flow, fracturing in these sediments may further enhance permeability and groundwater flow in these basin-fill aquifers by orders of magnitude.

Introduction

Rapid population growth and declining annual recharge to alluvial basin aquifers in the Nogales, Arizona, area has increased the demand for additional groundwater resources in the upper Santa Cruz basin (fig. 1). The geology and water resource potential of the Nogales Formation in the upper Santa Cruz basin has been poorly understood because limited geologic and hydrogeologic data have been collected from the formation (Erwin, 2007; Nelson, 2007); subsequently, the formation in the basin has not been widely developed for groundwater. Clear Creek Associates (2011) completed hydrogeologic investigations of the Santa Cruz River microbasins area for the City of Nogales, Ariz., to better understand the alluvial aquifers of this part of the basin, as many production wells for the city are in this area. Their studies included the collection of new controlled source audio-frequency magnetotelluric (CSMAT) data; drilling and logging of several exploratory boreholes; and the review of existing data, maps, and well data. The report concluded that the water produced by some of the wells may have been from the Nogales Formation, rather than from younger or older alluvial aquifers as previously reported, and that parts of the formation in the area may contain productive aquifers. Our new investigations also indicate that parts of the Miocene Nogales Formation may contain productive aquifers—new, deeper sources of groundwater for the Nogales, Ariz., area (Gray and others, 2014). Results of our studies are based primarily on detailed geologic mapping and geophysical interpretations of the formation in the Rio Rico and Nogales (Ariz.) 7.5’ quadrangles (figs. 1, 2) (Page and others, 2016).

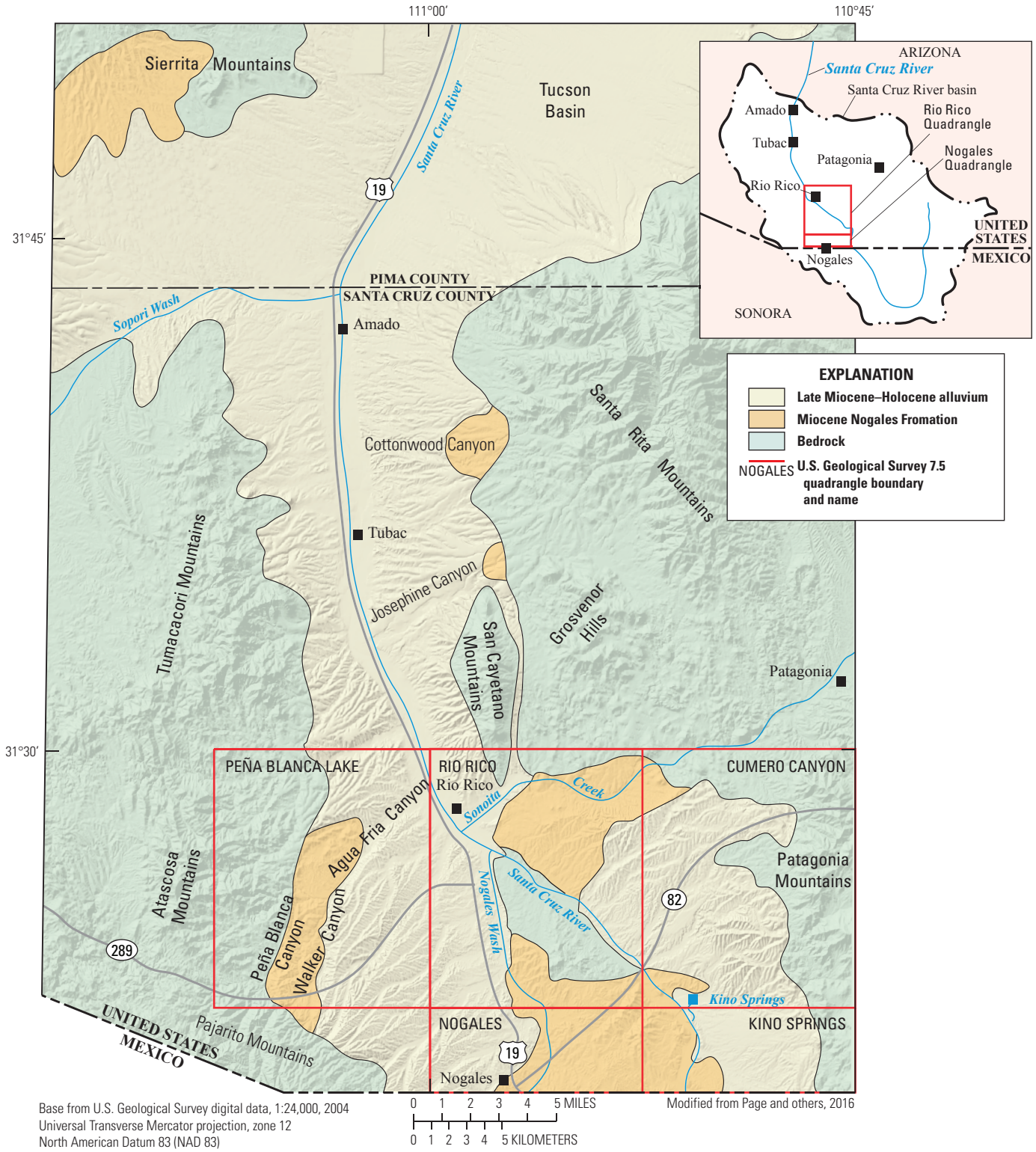

Figure 1. Map of the upper Santa Cruz basin area, showing major physiographic, geologic, and hydrologic features in the region. Inset map in upper right shows the boundary of the upper Santa Cruz River basin (dashed line) in relation to the Santa Cruz River and the Rio Rico and Nogales (Arizona) 7.5′ quadrangles (red).

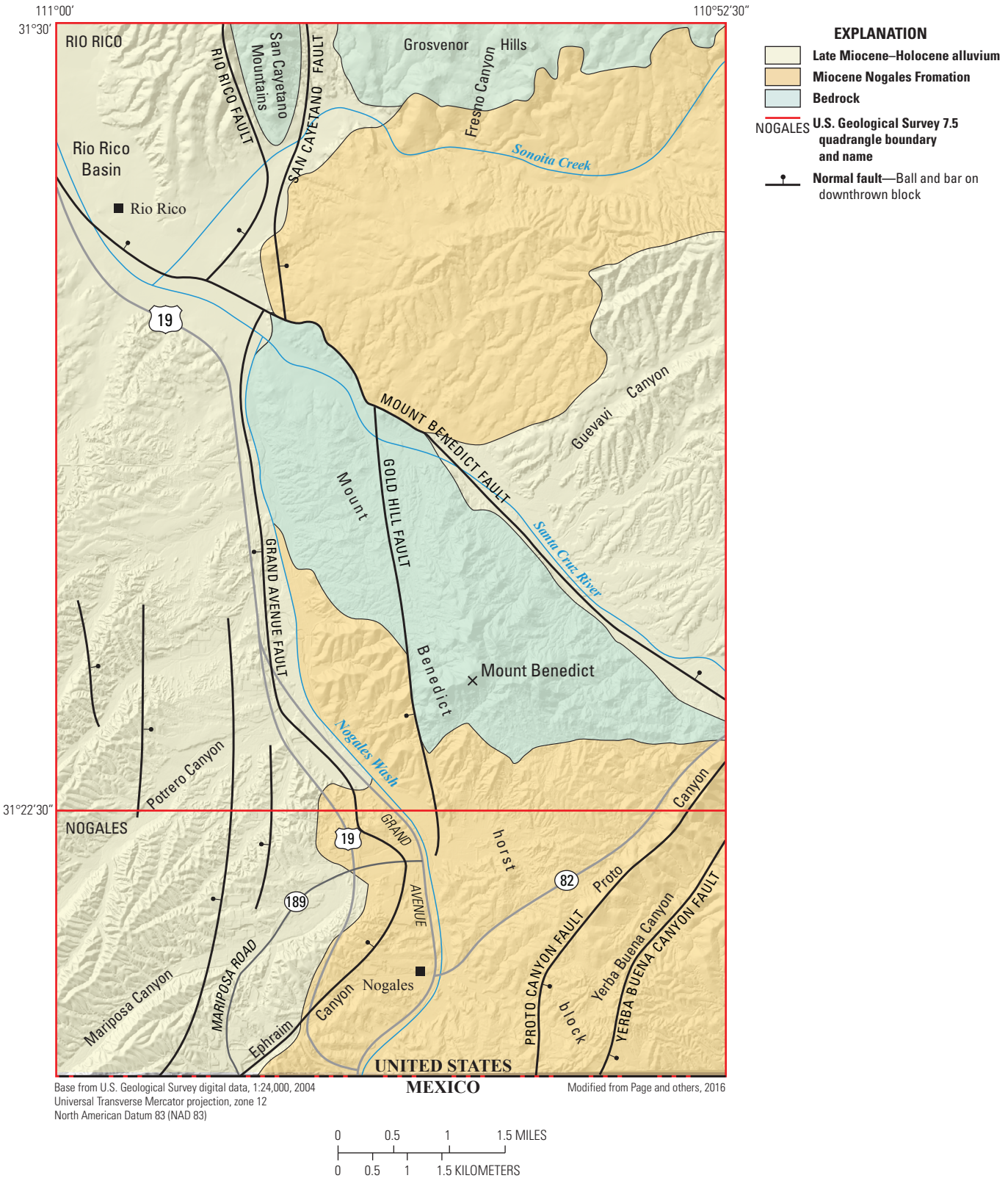

Figure 2. Map of the Rio Rico and Nogales (Arizona) 7.5′ quadrangles, showing major physiographic, geologic, and hydrologic features in the study area.

Nogales Formation Stratigraphy, Structure, and Basin Geometry

Stratigraphy

Page and others (2016) used detailed geologic mapping to significantly revise the stratigraphy of the Nogales Formation originally defined by Simons (1974). Based on mapping in the Rio Rico and Nogales (Ariz.) 7.5' quadrangles (figs. 1, 2), they defined three informal members—(from base to top) the Proto Canyon, Nogales Wash, and Mariposa members—named for their type areas where they are found in the Nogales, Ariz., area. Nogales Formation sediments were deposited by streams and debris flows on alluvial fans flanking the upper Santa Cruz basin and in playas in axial parts of the basin. The Nogales Formation unconformably overlies bedrock confining units, which include the Jurassic Quartz Monzonite of Mount Benedict; Cretaceous plutonic, volcanic, and sedimentary rocks; and Tertiary volcanic and plutonic rocks (Page and others, 2016). In the Nogales urban area, the formation generally overlies the Jurassic Quartz Monzonite of Mount Benedict, which was a local source area for sediments in the formation. Most of the sediments in the formation contain pumice and volcanic glass fragments, indicating that the Grosvenor Hills Volcanics and equivalent Tertiary volcanic rocks in the Tumacacori and Atascosa Mountains (fig. 1) were a more regional source of sediments for the formation. Because of the different source terrains, clastic units in the formation commonly contain mixtures of Oligocene volcanic rocks and Jurassic monzonite.

Proto Canyon Member

Basal parts of the Proto Canyon member consist of distinctive debris-flow conglomerate, which grades upward into arkose conglomerate and sandstone. The coarse debris-flow conglomerate is well exposed near the contact with the Jurassic monzonite, south of Mount Benedict, where it is well consolidated and clast-supported. These beds grade upward into distinctive weakly consolidated, reddish-orange sequences of alternating beds of arkose conglomerate and sandstone. The basal debris-flow conglomerate and arkose units are well exposed in the basin north of Proto Canyon and State Highway 82 and south of Mount Benedict (fig. 2) (Page and others, 2016), where their combined thickness is estimated to be about 100 to 250 meters (m) thick.

The lower units of the Proto Canyon member above the basal debris-flow conglomerate and arkose units consist of fining-upward cyclic sequences of volcaniclastic conglomerate, sandstone, and pumice siltstone; these units form massive cliffs in the Proto Canyon area, primarily along and south of State Highway 82. Middle parts of the member contain red and gray sandy and gravelly claystone, pale red arkosic conglomerate and sandstone, and yellowish-gray to brown volcaniclastic sandstone and conglomeratic sandstone; these units are best exposed in the Yerba Buena Canyon area (fig. 2). Lower and middle parts of the member are mostly exposed south of Proto Canyon and State Highway 82, extending southward across the international border into Sonora, Mexico.

The upper part of the Proto Canyon member consists mainly of pinkish-gray to yellowish-gray, moderately consolidated volcaniclastic sandstone and conglomerate; these rocks are mostly exposed in the Grand Avenue area, north of Mariposa Road (Page and others, 2016). Sandstone and conglomerate in the upper part of the member contain abundant monzonite clasts, reflecting localized erosion of the Quartz Monzonite of Mount Benedict. The thickness of the Proto Canyon member is highly variable, but maximum thickness is about 450 m.

The Proto Canyon member is also exposed in the Sonoita Creek area, where it laps onto the Grosvenor Hills Volcanics in the southern Grosvenor Hills. In this area, the lower part of the unit is pinkish-gray, cliff-forming to ledgy volcaniclastic conglomerate containing clasts and grains of mostly white and red porphyritic volcanic rocks, brownish-gray rhyodacite, pumice, and latite derived from the Grosvenor Hills Volcanics. The upper part of the unit is fine-grained, moderately sorted volcaniclastic sandstone and some conglomeratic sandstone, which weathers to distinctive rounded ledges. These rocks are moderately fractured in the Sonoita Creek area.

Nogales Wash Member

The Nogales Wash member is only present in the Nogales 7.5' quadrangle (Page and others, 2016), and exposures are limited to south of Mariposa Road, extending from Ephraim Canyon to about 4 kilometers (km) east of Grand Avenue (fig. 2). Distribution of the member, combined with on-lapping relations with the lower part of the Proto Canyon member, suggests the Nogales Wash member sediments were deposited in a paleovalley eroded into the Proto Canyon member, coincident with the modern-day Nogales Wash (Page and others, 2016). The Nogales Wash member is estimated to be as much as 150 m thick in the deeper subbasins of the upper Santa Cruz basin (Page and others, 2016). The basal 20–30 m contains distinctive massive cliffs of yellowish-gray to pinkish-gray, moderately consolidated volcaniclastic sandstone and conglomeratic sandstone, and most of the other parts of the member contain alternating beds of thin- to thick-bedded volcaniclastic sandstone and conglomeratic sandstone. Rocks of the Nogales Wash member are pervasively fractured in the upper Santa Cruz basin.

Mariposa Member

The Mariposa member is exposed in the Mariposa Road and Interstate 19 areas, where it contains alternating beds of conglomerate, conglomeratic sandstone, sandstone, siltstone, and claystone; the member is generally less consolidated and more calcareous compared to the other members. In the Mariposa Road area, a 60-m-thick massive claystone unit represents playa deposits in axial parts of the basin (Page and others, 2016). The claystone may be a significant confining

unit in the basin, but more subsurface data need to be collected to determine its lateral continuity and thickness. The member is widely exposed in the basin south of Sonoita Creek, east of the Santa Cruz River, and north of Guevavi Canyon, where it contains pinkish-gray alternating beds of sandstone, siltstone, and claystone, like in the Mariposa Road area. These units, however, are generally thinner bedded and finer grained. The Mariposa member is also exposed southeast of State Highway 82 and just north of the international border, where lower parts of the member consist of conglomeratic sandstone, fine-grained sandstone, and thin, discontinuous lava flows 3–5 m thick. One basalt sample was dated and yielded a $^{40}Ar/^{39}Ar$ (argon-argon) age of 11.67±0.09 mega-annum (Ma) (Cosca and others, 2013; Page and others, 2016); this date provides an absolute minimum age for the Nogales Formation.

Structure

Structural features in the Nogales, Ariz., area primarily formed during early to late Miocene extensional deformation, which occurred in southern Arizona mostly from 20 to 10 Ma (Menges, 1981; Menges and McFadden, 1981; Menges and Pearthree, 1989). Extensional deformation was broadly contemporaneous with deposition of the Nogales Formation, based on observations that all members of the formation are faulted and exhibit abundant intra-formational faults and fractures and moderately to steeply inclined bedding dips. Extensional faulting in the area lasted until late Miocene time, based on the observation that faults only cut the very oldest late Miocene basin-fill deposits (postdating Nogales Formation deposition) and that deposits from the Pliocene through the Holocene are undeformed (Page and others, 2016).

The main structural feature in the study area is the Mount Benedict horst block (fig. 2) (Page and others, 2016), a triangular zone of uplifted Quartz Monzonite of Mount Benedict (Jurassic) and overlying members of the Nogales Formation. The fault bounding the east side of the horst block is the Mount Benedict fault, the major fault in the region which controls the location of the course of the Santa Cruz River from the Rio Rico area southward into Mexico. The fault is exposed northwest of Guevavi Canyon and southeast of Sonoita Creek (Page and others, 2016), where it dips northeast and offsets rocks of the Jurassic monzonite and overlying Salero Formation in the footwall, against the Mariposa member of the Nogales Formation in the hanging wall. Other known exposures of the fault are in the Cumero Canyon 7.5’ quadrangle (fig. 1), southeast of the intersection of State Highway 82 and the Santa Cruz River. At this location, the fault juxtaposes clayey arkosic conglomerate of the Proto Canyon member in the footwall, against volcaniclastic sandstone of the Mariposa member in the hanging wall.

The Grand Avenue fault (fig. 2) forms the west margin of the Mount Benedict horst block. The fault is exposed just south of Mariposa Road and west of Grand Avenue, where it strikes northeast and dips northwest. The southern part of the fault juxtaposes rocks of the Nogales Wash member against those of the Mariposa member of the Nogales Formation, but north of Mariposa Road, rocks of the Mariposa member are faulted against those of the Proto Canyon member and the Quartz Monzonite of Mount Benedict. Several other concealed faults interpreted from airborne transient electromagnetic data and other geophysical data are mapped west of the Grand Avenue fault (Page and others, 2016); these faults and the Grand Avenue fault form a complex graben system in the subsurface west of the horst block (fig.2).

Basin Geometry

Basin Evolution

Geophysical data were interpreted to determine basin geometry and thickness of the Nogales Formation and younger alluvial aquifers and to identify target areas (deep subbasins) which may prove to be productive aquifers. The upper Santa Cruz depositional basin includes the area west of the Patagonia Mountains, south of the Grosvenor Hills, west of the San Cayetano and Santa Rita Mountains, and east of the Atascosa and Tumacacori Mountains (fig. 1) and extends southward into Sonora, Mexico. The basin geometry is complex because of a highly irregular erosion surface that predates the Nogales Formation and developed on Jurassic and Cretaceous rocks (Page and others, 2016), which were deformed by episodes of Miocene Basin and Range extension and older pre-Tertiary deformational events, most notably Cretaceous plutonism and faulting related to the Laramide orogeny (Simons, 1974).

Sediments of the Proto Canyon member of the Nogales Formation represent initial deposition in the southern part of the upper Santa Cruz basin and were laid down across an area coincident with that of the modern day basin. During deposition of the Proto Canyon member, Mount Benedict (fig. 2) was likely a paleotopographic high near the center of the basin, based on coarse debris-flow conglomerate at the base of the Proto Canyon member shed off the flanks of Mount Benedict. The horst block experienced multiple stages of uplift during deposition of the Nogales Formation based on unconformities bounding each member of the formation and onlapping relations between the Proto Canyon member and the Nogales Wash and Mariposa members (Page and others, 2016).

Uplift of the Mount Benedict horst block occurred during and (or) following deposition of the Proto Canyon member to expose the basal debris-flow conglomerate and to further compartmentalize the southern part of the upper Santa Cruz basin into two main basins: one west of the horst block and east of the Atascosa and Tumacacori Mountains, and another east of the horst block and Santa Cruz River, south of the Grosvenor Hills, and west of the Patagonia Mountains (figs. 1, 2). Further faulting and uplift of the horst block continued throughout and following deposition of the Nogales Formation, based on the observation that all members are fractured and faulted, that major faults cut the very oldest part of alluvial basin-fill deposits that postdate the Nogales Formation and overlie it, and that sediments from the Pliocene through the Holocene are generally undeformed.

Depth to Bedrock Maps

Based on geophysical interpretations, we constructed depth to bedrock maps to delineate subsurface contacts and fault boundaries between Jurassic and Cretaceous bedrock confining units and the overlying Nogales Formation. The maps also define the geometry of deep subbasins (fig. 3) that contain aquifers of the Nogales Formation and overlying younger basin fill and alluvium. The subbasins are about 500 to 800 m deep and contain thick sections of fractured Nogales Formation sediments; they are considered target areas for additional groundwater resources in the upper Santa Cruz basin.

Gettings and Houser (1997) used complete Bouguer gravity anomaly data to obtain a preliminary depth to bedrock for the Santa Cruz basin. We used the 1996 Patagonia aeromagnetic survey (Sweeney and Hill, 2001) to produce a depth to bedrock map with a higher spatial resolution than preliminary maps in the Rio Rico and Nogales (Ariz.) 7.5' quadrangles. Analysis of the aeromagnetic data included three methods to estimate depth to bedrock: Euler deconvolution, horizontal gradient magnitude, and analytic signal. The final depth to bedrock map was produced by choosing the maximum depth from each of the three methods at a given location and combining all maximum depths. The resulting map (fig. 3) provides a much more detailed description of depth to bedrock in the upper Santa Cruz basin study area than had previously existed and shows the location and geometry of the six deep subbasins (fig. 3).

Results of Porosity, Bulk Density, Saturated Hydraulic Conductivity, and Fabric Analyses for the Nogales Formation

A total of 22 sandstone samples were taken from the Nogales Formation for analysis (fig. 4, table 1). Of those samples, 14 samples were analyzed for total and effective porosity and bulk density (table 2), and 13 samples were analyzed for saturated hydraulic conductivity (SHC) (table 3). For fabric analyses, thin sections were examined for 21 samples (appendix 1), and 5 samples were investigated using scanning electron microscope (SEM) and x-ray diffraction (XRD) methods. Table 1 lists all samples analyzed and identifies the location, formation member, and type or types of analyses reported for each, as well as any associated figures. All samples were collected from outcrops, and all samples are sandstone. The values obtained, therefore, are not representative of the full spectrum of lithostratigraphic units in the Nogales Formation, although sandstone is the most abundant rock type in the formation. Our analyses were limited to sandstones because other units in the formation, including clay-rich units in the Mariposa and Proto Canyon members, were typically too weakly consolidated for porosity and SHC analyses. While both total and effective porosity was measured, effective porosity (the amount of mutually interconnected pore space) is key to hydrologic investigations, so all porosity values discussed henceforth represent only effective porosity.

Effective porosity values from the Nogales Formation range from 16 to 42 percent (table 2). The highest porosity was from sandstone in the upper part of the Proto Canyon member (fig. 2–1*B*), and the lowest from sandstone in the lower part of the Mariposa member (fig. 2–1*F*). Gettings and Houser (1997) calculated a porosity of 16 percent for rocks equivalent to the Nogales Formation, based on a combination of downhole gravimeter data, grain density measurements of cuttings, and surface gravimetric profiles. Their porosity value is low compared to most of the results from our analyses.

Bulk density in the formation ranges from 1.60 grams per cubic centimeter (g/cm^3) to as much as 2.47 g/cm^3 (table 2); the highest value is from moderately consolidated sandstone near the base of the Nogales Wash member (fig. 2–1*A*), and the lowest is from sandstone in the lower part of the Mariposa member (fig. 2–1*A*). Gettings and Houser (1997) calculated saturated bulk density for rocks equivalent to the Nogales Formation, based on downhole gravimetric measurements; they reported values from 2.00 to 2.38 g/cm^3, which are in agreement with most of the values determined by our analyses.

Values for SHC for the formation are wide ranging, from 4 to 57 centimeters per day (cm/d) (table 3). Both the highest and lowest SHC are from the upper part of the Proto Canyon member (fig. 2–1*C*). Published SHC data for the Nogales Formation are sparse, but Erwin (2007) reported composite values of 0.4 and 0.5 feet per day (ft/d) (12 and 15 cm/d) from aquifer tests completed in wells penetrating alluvium that postdates the Nogales Formation and in the Nogales Formation in the Kino Springs area (fig. 1). Nelson (2007) reported hydraulic conductivities for the Nogales Formation in the upper Santa Cruz basin at 0.17 ft/d (5.1 cm/d), 0.3 ft/d (9.1 cm/d), and 0.43 ft/d (13.1 cm/d), based on aquifer tests west of Tubac, Ariz. (fig. 1).

Fabric analyses included petrographic, SEM, and XRD methods. Twenty-one thin sections from all members of the Nogales Formation were examined and described (appendix 1). Thin sections show that framework grains generally consist of quartz, feldspar, biotite, hornblende, porphyritic volcanic clasts with biotite and hornblende, quartz-biotite monzonite porphyritic clasts, pumice and altered volcanic glass, small scattered opaque minerals including ilmenite, iron oxide, and manganese oxide. Approximately half of the thin sections have a matrix of mostly pumice and glass, and half contain combinations of pumice, glass, silt, and clay (appendix 1). Samples with a predominantly silt and clay matrix generally have lower porosity and SHC (porosities at 26 percent and lower; SHC 15–33.4 cm/d; tables 2, 3) compared to samples with a mostly pumice and glass matrix, which have higher porosity and SHC as well as wider ranges of porosity (20–42 percent; table 2) and SHC (5.6–57 cm/d; table 3).

Most sandstone in the formation is poorly sorted, but some is moderately sorted and fine grained. Only two such samples were analyzed, and both have low porosity values

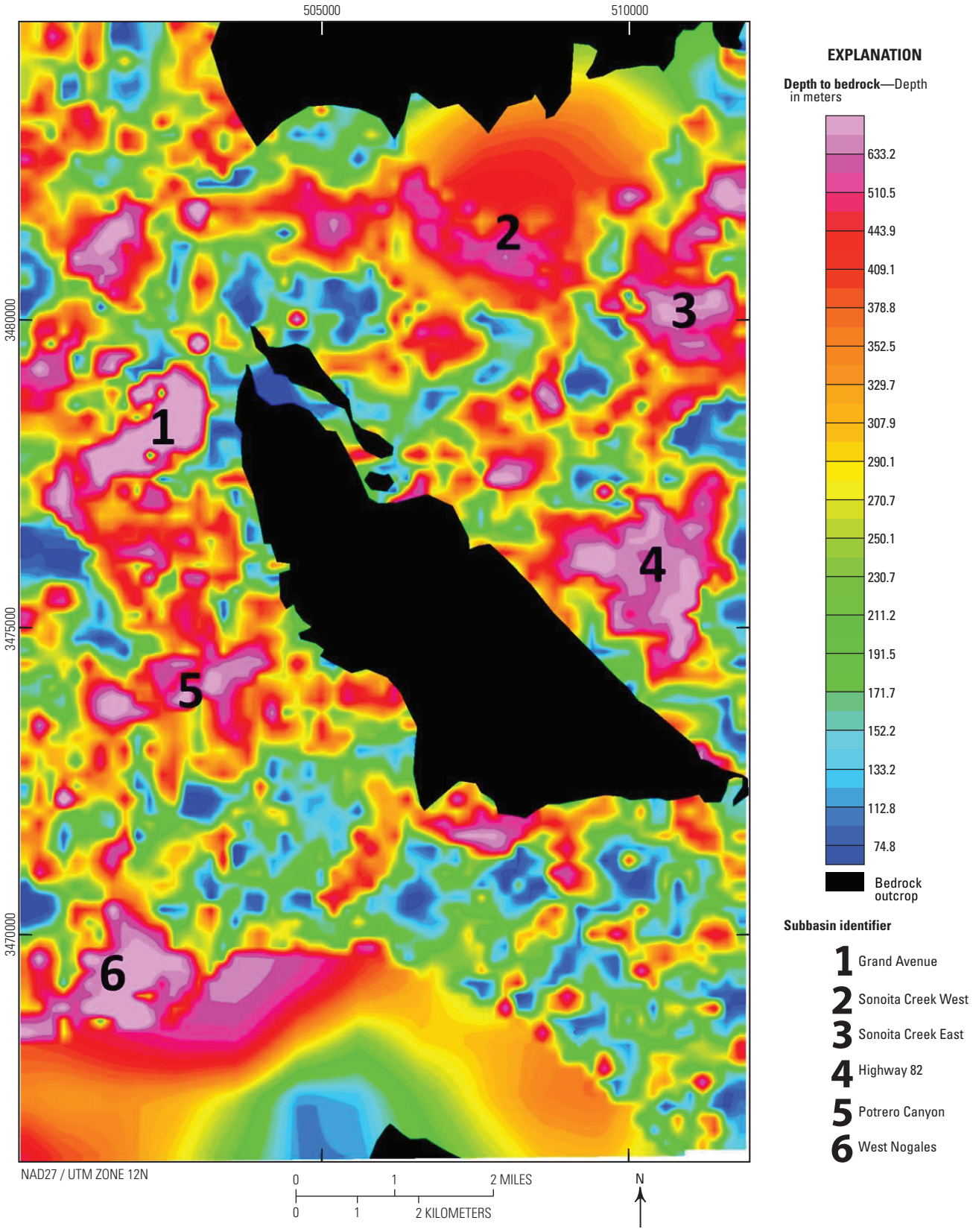

Figure 3. Depth to bedrock in the Rio Rico and Nogales (Arizona) 7.5′ quadrangles (study area shown in figure 2). Deeper subbasins in the area are numbered: (1) Grand Avenue subbasin, (2) Sonoita Creek West subbasin, (3) Sonoita Creek East subbasin, (4) Highway 82 subbasin, (5) Potrero Canyon subbasin, and (6) West Nogales subbasin. Black areas indicate bedrock outcrops.

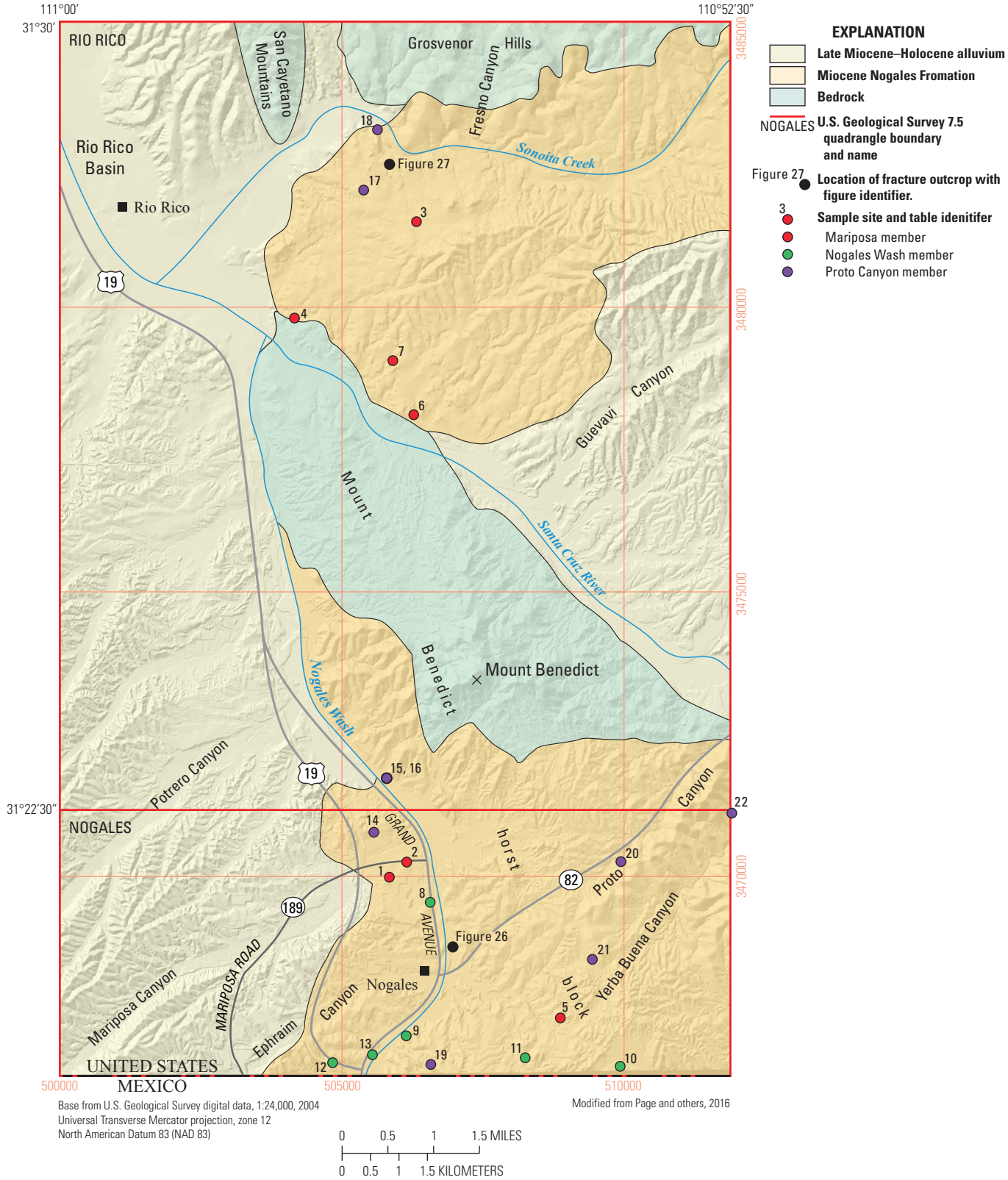

Figure 4. Locations of Nogales Formation samples analyzed in this study. Sample site identifiers correspond to entries in tables 1–3.

Table 1. Description of all samples from the Nogales Formation analyzed in this study.

[Columns include (from left to right) (1) sample site identifiers keyed to figure 4, (2) original field sample number, (3) Universal Transverse Mercator (UTM) easting and northing, (4) Nogales Formation member name, (5) types of analyses performed, and (6) associated figure (outcrop photograph, thin section, or SEM image). SHC, saturated hydraulic conductivity; phys. prop., total and effective porosity and bulk density; TS, thin section; SEM, scanning electron microscope; XRD, x-ray diffraction]

Sample site	Sample number	UTM Zone 12		Nogales Formation member	Analyses	Figure number
		Easting	Northing			
1	10-RP-2	505843	3469986	Mariposa	SHC, phys. prop., TS, SEM, XRD	22
2	10-RP-9	506150	3470251	Mariposa	TS	
3	RP-12-9	506324	3481500	Mariposa	TS	
4	RP-12-11	504162	3479807	Mariposa	phys. prop., TS	20, 21
5	RP-12-19a	508873	3467513	Mariposa	SHC, phys. prop., TS	
6	RP-12-27	506276	3478109	Mariposa	SHC, phys. prop., TS, SEM, XRD	18, 19
7	RP-12-29	505905	3479060	Mariposa	TS	
8	10-RP-4	506567	3469545	Nogales Wash	SHC, TS	16
9	10-RP-10	506142	3467200	Nogales Wash	phys. prop., TS	13
10	RP-12-15	509934	3466664	Nogales Wash	SHC, TS	
11	RP-12-16	508250	3466814	Nogales Wash	TS	
12	RP-12-24	504837	3466727	Nogales Wash	phys. prop., TS	
13	RP-12-46	505543	3466868	Nogales Wash	SHC, phys. prop., TS	14, 15
14	10-RP-3	505568	3470775	Proto Canyon	SHC, phys. prop., TS, SEM, XRD	9, 10
15	RP-12-4a	505796	3471725	Proto Canyon	SHC, phys. prop., TS	
16	RP-12-4b	505796	3471725	Proto Canyon	SHC	
17	RP-12-7	505388	3482056	Proto Canyon	SHC, phys. prop., TS, SEM, XRD	11, 12
18	RP-12-8	505632	3483117	Proto Canyon	TS	
19	RP-12-14	506579	3466697	Proto Canyon	phys. prop., TS	
20	RP-12-21	509952	3470259	Proto Canyon	SHC, phys. prop., TS, SEM, XRD	5, 6, 7
21	RP-12-32	509441	3468542	Proto Canyon	SHC, phys. prop., TS	
22	RP-12-42a	511913	3471111	Proto Canyon	SHC, phys. prop., TS	

Table 2. Total and effective porosity and bulk density for sandstone samples from the Nogales Formation.

[Analyses performed at the U.S. Geological Survey Hydrologic Research Laboratory in Sacramento, California. Sample sites are shown in figure 4. %, percent; g/cm^3, grams per cubic centimeters]

Sample site	Sample number	Nogales Formation member	Total porosity (%)	Effective porosity (%)	Bulk density (g/cm^3)
1	10-RP-2	Mariposa	29	24	1.6
4	RP-12-11	Mariposa	23	16	2.07
5	RP-12-19a	Mariposa	25	21	2.23
6	RP-12-27	Mariposa	42	36	2.37
9	10-RP-10	Nogales Wash	37	31	2.47
12	RP-12-24	Nogales Wash	28	22	1.86
13	RP-12-46	Nogales Wash	25	22	1.76
14	10-RP-3	Proto Canyon	49	42	2.0
15	RP-12-4a	Proto Canyon	35	26	2.41
17	RP-12-7	Proto Canyon	26	22	1.94
19	RP-12-14	Proto Canyon	23	20	2.13
20	RP-12-21	Proto Canyon	39	32	2.2
21	RP-12-32	Proto Canyon	34	29	1.78
22	RP-12-42a	Proto Canyon	31	24	1.79

Table 3. Saturated hydraulic conductivity for sandstone samples from the Nogales Formation.

[Analyses performed at the U.S. Geological Survey Hydrologic Research Laboratory in Sacramento, California. Sample sites are shown in figure 4. cm/s, centimeters per second; cm/d, centimeters per day]

Sample site	Sample number	Nogales Formation member	Saturated hydraulic conductivity	
			(cm/s)	(cm/d)
1	10-RP-2	Mariposa	3.9×10^{-4}	33.4
5	RP-12-19a	Mariposa	6.4×10^{-5}	5.6
6	RP-12-27	Mariposa	3.8×10^{-4}	32.7
8	10-RP-4	Nogales Wash	4.3×10^{-4}	38
10	RP-12-15	Nogales Wash	3×10^{-4}	26
13	RP-12-46	Nogales Wash	2.7×10^{-4}	23.6
14	10-RP-3	Proto Canyon	4.9×10^{-5}	4.0
15	RP-12-4a	Proto Canyon	1.7×10^{-4}	15
16	RP-12-4b	Proto Canyon	5.0×10^{-4}	43
17	RP-12-7	Proto Canyon	6.7×10^{-4}	57
20	RP-12-21	Proto Canyon	4.1×10^{-4}	35.3
21	RP-12-32	Proto Canyon	5.7×10^{-5}	4.9
22	RP-12-42a	Proto Canyon	1.7×10^{-4}	14.3

compared to other samples and wide-ranging SHC, from 5.6 to 57 cm/d. About 6 samples from the formation contained fractures, and all were open fractures. Samples with fractures have wide-ranging porosity (26–42 percent) and low SHC (4–15 cm/d). Fractured sandstones also have higher bulk densities compared to other samples, ranging from 2.0 to 2.47 g/cm^3. Most samples from the Mariposa member contain secondary calcite cement, which partially fills intercrystalline pore space. Samples with calcite cement have wide-ranging porosity (16–36 percent) and SHC (15–33.4 cm/d).

Five samples from the Nogales Formation were analyzed using SEM and XRD methods to identify and describe clay composition in the formation. Analyses indicate that most of the samples contain the zeolite clinoptilolite and varying amounts of mixed-layer clay. X-ray diffraction analyses verified clinoptilolite as the only zeolite in Nogales Formation samples as well as the presence of mixed-layer smectite and illite clay and some kaolinite. Clinoptilolite likely precipitated in pore space of the Nogales Formation sediments during post-depositional basin diagenesis, similar to processes of sedimentary basin diagenesis described by Gotardi and Galli (1985), whereby clinoptilolite is precipitated from the dissolution of silica-rich volcanic glass as it reacts with alkaline meteoric groundwater. In most samples, clinoptilolite crystals occur as disseminated microcrystalline aggregates, filling intercrystalline pore space. The presence of clinoptilolite, in addition to mixed-layer smectite and illite clays, partly accounts for the moderately high porosity in the formation, which ranges from 16 to as much as 42 percent. Iijima (2001) reported similar porosity values of 20 to 40 percent for clinoptilolite-bearing Cenozoic to Mesozoic basinal volcaniclastic sandstones in Japan, and these rocks form the major commercial petroleum reservoirs in those basins. Scanning electron microscope and x-ray diffraction methods show that samples with greater clinoptilolite and lesser smectite have high porosity (32–36 percent) and SHC (32.7–35.3 cm/d) in narrow ranges. Conversely, samples with abundant smectite and minor clinoptilolite have wide-ranging porosity, with values ranging from a low of 24 percent to the maximum value for the entire formation at 42 percent, and values for SHC that range from the lowest for the formation at 4 cm/d to the maximum for the formation at 57 cm/d.

Discussion of Analyses by Nogales Formation Member

Proto Canyon Member

The Proto Canyon member of the Nogales Formation is lithologically diverse compared to the other members and, in turn, has wide-ranging values for porosity, bulk density, and SHC. The highest porosity is from sandstone in the upper part of the member, and the lowest from the middle part (fig. 2–1*B*). The highest SHC is also from sandstone in the upper part of the member, and the lowest from the middle and upper parts (fig. 2–1*C*). The highest bulk density (fig. 2–1*A*) is from moderately consolidated sandstone in the upper part of the member (2.41 gm/cm^3), and the lowest densities (1.78 and 1.79 g/cm^3) from samples in the middle part, which contains more claystone than other parts of the member.

The lower part of the member (above the basal conglomerate and arkose) contains fining-upward cyclic sequences of conglomerate, sandstone, and laminated pumice siltstone (fig. 5). Sandstone from these sequences (sample RP-12-21)

Figure 5. Cyclic fining-upward sequences in the lower part of the Proto Canyon member in Proto Canyon. Cycles generally consist of volcaniclastic conglomerate (vc) and conglomeratic sandstone (vcs) capped by white pumice siltstone (ps); these sequences also contain some debris-flow conglomerate (dfc). Sandstone from these sequences (sample RP-12-21; site 20 on fig. 4) has relatively high effective porosity at 32 percent and a saturated hydraulic conductivity value of 35.3 centimeters per day. Thin sections (fig. 6) show that these rocks contain moderate amounts of moldic and minor intercrystalline pore space.

has relatively high porosity at 32 percent, bulk density at 2.2 g/cm^3, and SHC at 35.3 cm/d. Thin sections show a mostly pumice matrix with moderate amounts of open pore space (fig. 6). Scanning electron microscope and x-ray diffraction analyses for this sample indicated high amounts of clinoptilolite (fig. 7) and minor smectite.

Middle parts of the member, which are exposed primarily south of Proto Canyon and State Highway 82 and extending to the international border (fig. 2), contain alternating arkosic conglomerate, gravelly claystone, and sandstone beds (fig. 8). The middle part of the member is less fractured than the other parts, probably because of higher amounts of clay. Sandstones from the middle part of the member (samples RP-12-14, RP-12-42a, and RP-12-32) have low to intermediate porosity of 20, 24, and 29 percent, respectively. Bulk density is low for samples RP-12-32 (1.78 g/cm^3) and RP-12-42a (1.79 g/cm^3) and intermediate for sample RP-12-14 (2.13 g/cm^3). The lowest porosity in the middle part is from sandstone that is interbedded with sandy claystone and siltstone beds (sample RP-12-14), and thin sections show moderate moldic pore space within pumice grains, minor intercrystalline pore space, and a combination pumice, silt, and clay matrix. Samples RP-12-32 and RP-12-42a, in addition to having low to intermediate porosity, also have low SHC at 4.9 cm/d and 14.3 cm/d, respectively. Similar to sample RP-12-14 above, both samples have a combination pumice, silt, and clay matrix and moderate moldic and minor intercrystalline pore space.

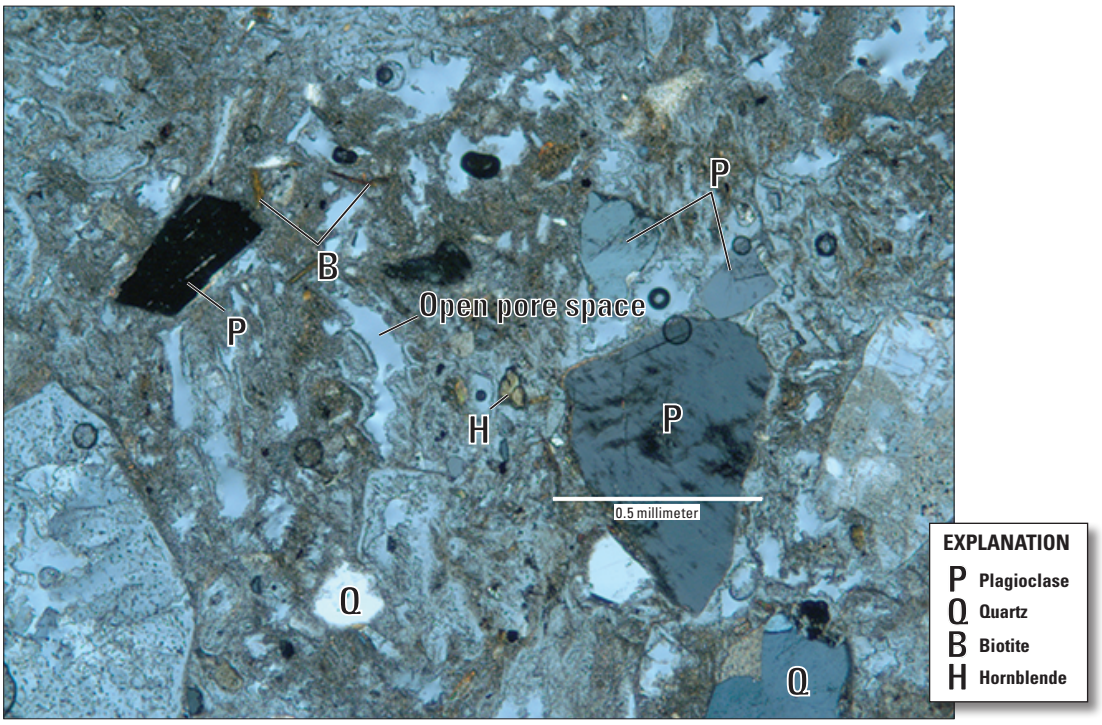

Figure 6. Thin section of sandstone (sample RP-12-21; site 20 on fig. 4) from the lower part of the Proto Canyon member at Proto Canyon showing a predominantly pumice fragment matrix and mostly plagioclase, quartz, biotite, and hornblende framework grains. See figure 5 for photograph of outcrop. Plane polarized light; open pore space is in light blue (one example indicated on image). (mm, millimeter)

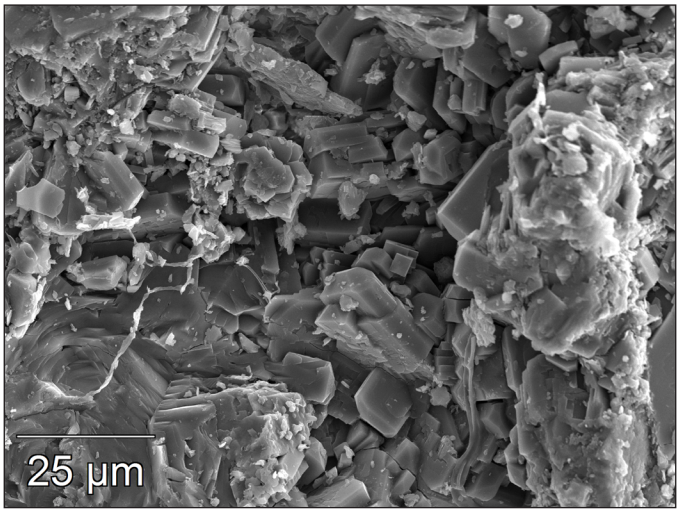

Figure 7. Scanning electron microscope image of sandstone (sample RP-12-21; site 20 on fig. 4) from the lower part of the Proto Canyon member at Proto Canyon showing clinoptilolite in pore space. Clinoptilolite crystals are generally less than 25 micrometers (µm) in size. See figure 5 for photograph of outcrop. Image shows primarily clinoptilolite; smectite and illite clay is likely present, but precise identification of clay could not be determined from these analyses.

Figure 8. Red and light gray gravelly claystone (below black line) and overlying gray volcaniclastic sandstone beds (above black line) in the middle part of the Proto Canyon member in Yerba Buena Canyon. Exposed part of gray sandstone bed above black line at far right is about 0.5 meter thick. These rocks (samples RP-12-14, RP-12-42a, and RP-12-32; sites 19, 22, and 21 on fig. 4) have low to intermediate porosity values at 20, 24, and 29 percent and low saturated hydraulic conductivity values at 4.9 and 14.3 centimeters per day.

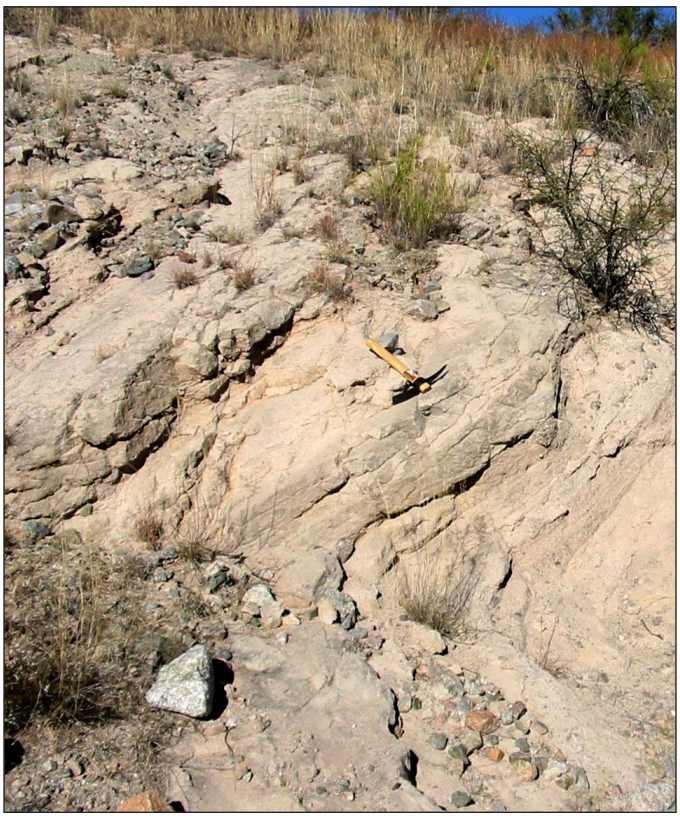

Figure 9. Pinkish-gray volcaniclastic sandstone in the uppermost part of the Proto Canyon member between Interstate 19 and Grand Avenue, north of Mariposa Road; pick for scale. Sandstone from this location (sample 10-RP-3; site 14 on fig. 4) has the highest effective porosity for the entire Nogales Formation at 42 percent but also has the lowest saturated hydraulic conductivity for the formation at 4.0 centimeters per day.

Sample RP-12-32 also has abundant silt and clay layers, which may partly explain the low SHC value, the second lowest of all samples in the formation.

The upper part of the Proto Canyon member is moderately consolidated sandstone (sample 10-RP-3; fig. 9) and has the highest effective porosity (42 percent) of all samples from the entire Nogales Formation. Thin sections show abundant intercrystalline, moldic, and fracture pore space, as well as a pumice and volcanic glass fragment matrix. This rock has the lowest SHC of all Nogales Formation samples (4.0 cm/d) and contradicts the observation that many sediments with high porosity generally have corresponding high hydraulic conductivity (Pryor, 1973; Freeze and Cherry, 1979). X-ray diffraction analyses indicate that the rock has very high amounts of smectite and minor amounts of clinoptilolite. Scanning electron microscope analyses show abundant smectite and illite clay coating the surfaces of tabular-shaped clinoptilolite crystals, in addition to abundant interspersed fibrous, organic material (fig. 10). A possible explanation for the very high

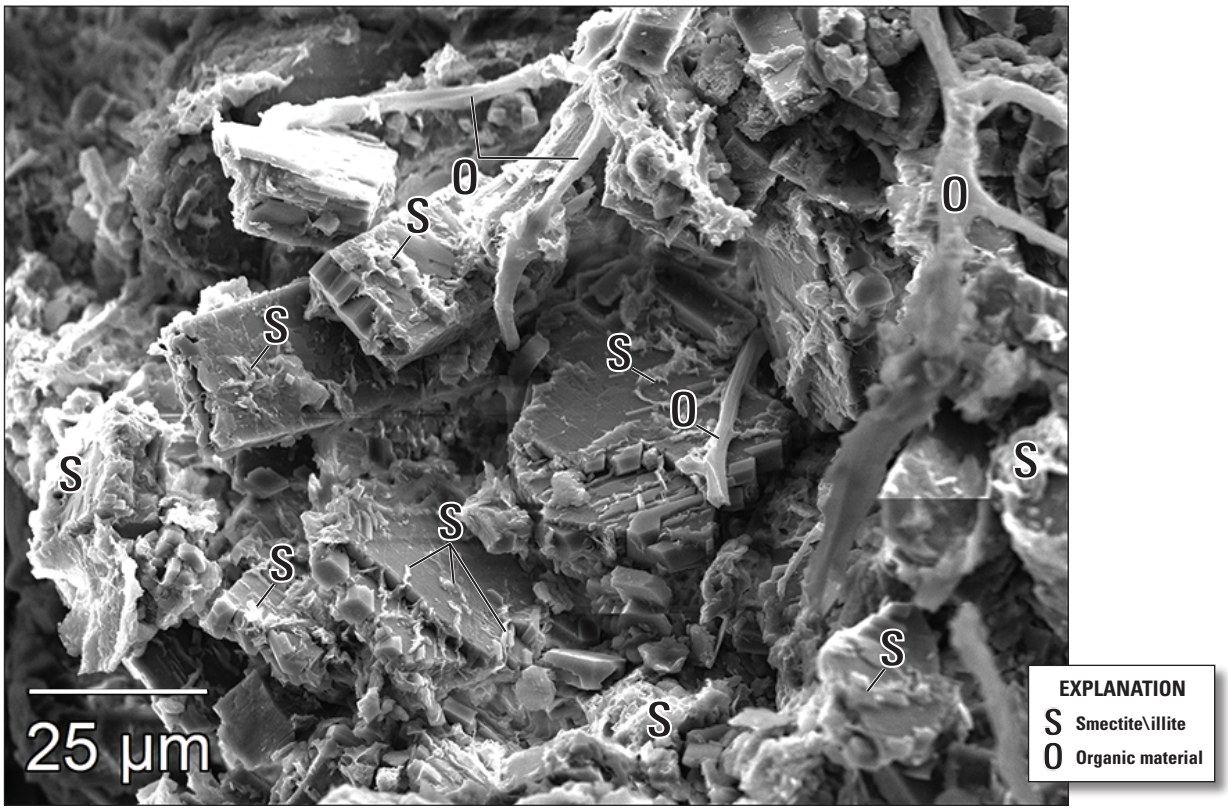

Figure 10. Scanning electron microscope image of sandstone (sample 10-RP-3; site 14 on fig. 4) from the uppermost part of the Proto Canyon member between Interstate 19 and Grand Avenue, north of Mariposa Road, showing clinoptilolite in pore space. Note the abundant smectite/illite clay coating tabular clinoptilolite and the abundant interspersed fibrous organic material. Clinoptilolite crystals are generally 25 micrometers (µm) or greater in size. See figure 9 for photograph of outcrop.

porosity and extremely low SHC is that clay coatings and organic material clog up pore space to inhibit SHC. In comparison with sample 10-RP-3, sample RP-12-21 in the lower part of the Proto Canyon member (fig. 5) has moderately high porosity (32 percent) and SHC (35.3 cm/d). Further, SEM and XRD analyses indicate that this rock contains abundant clinoptilolite and minor smectite; the clinoptilolite crystals appear "cleaner" (fig. 7) and lack the clay coatings and organic material observed in sample 10-RP-3.

We analyzed a coarse-grained conglomeratic sandstone (sample RP-12-4a) and a fine-grained sandstone (sample RP-12-4b) from the upper part of the Proto Canyon member at the same location and stratigraphic horizon. The coarse-grained conglomeratic sandstone has relatively low porosity (26 percent) and SHC (15 cm/d), and thin sections show a predominantly clay and silt matrix and moderate amounts of secondary calcite filling intercrystalline pore space. The coarse-grained conglomeratic sandstone has the highest bulk density for the Proto Canyon member at 2.41 g/cm^3, and thin sections show abundant fracture porosity, which reflects greater consolidation in the sandstone of the upper part of the member compared to the middle and lower parts of the member. The fine-grained sandstone (sample RP-12-4b) has significantly higher SHC at 43 cm/d (the second highest SHC of all Nogales Formation samples), but no porosity or fabric data were available to interpret and explain the higher SHC.

Sample RP-12-7, from sandstone in the upper part of the Proto Canyon member in the Sonoita Creek area (fig. 11), has relatively low porosity (22 percent) but has the highest SHC (57 cm/d) for the entire Nogales Formation. Thin sections show the rock is moderately sorted and fine grained and has a pumice and glass matrix, moderate moldic pore space, and moderate to abundant amounts of micro-intercrystalline pore space between small, angular, disaggregated pumice and glass fragments. X-ray diffraction analyses indicate that the sample contains abundant clinoptilolite and smectite, and SEM analyses show moderate amounts of open pore space (fig. 12), which may partly explain the high SHC.

Figure 11. Fine-grained, moderately sorted volcaniclastic sandstone in the upper part of the Proto Canyon member in the Sonoita Creek area. Sandstone from this unit (sample RP-12-7; site 17 on fig. 4) has a low porosity at 22 percent and the highest saturated hydraulic conductivity for the entire Nogales Formation at 57 centimeters per day.

Nogales Wash Member

The Nogales Wash member typically contains ledgy to cliff-forming sandstone and conglomeratic sandstone and generally lacks claystone beds, unlike the other formation members. Three samples from the member analyzed for physical properties have low to intermediate porosity at 22, 22, and 31 percent (samples RP-12-24, RP-12-46, and 10-RP-10, respectively). The highest porosity is from sandstone in the cliff-forming lower part of the member (fig. 2–1*D*); these rocks also have the highest bulk density for the entire formation (fig. 2–1*A*) and are pervasively fractured because of their brittleness from a higher degree of consolidation and lesser amounts of claystone compared to the other members. Saturated hydraulic conductivity for the member is intermediate and ranges from 23.6 to 38 cm/d; the highest SHC is from units in the middle part of the member (fig. 2–1*E*).

Sample 10-RP-10 has the highest porosity in the member (31 percent) and is from moderately consolidated sandstone in the lower cliff-forming part of the member (fig. 13). Thin sections show abundant fracture porosity and moderate amounts of moldic and intercrystalline pore space. Sample 10-RP-10 has the highest bulk density (2.47 g/cm^3) for the entire

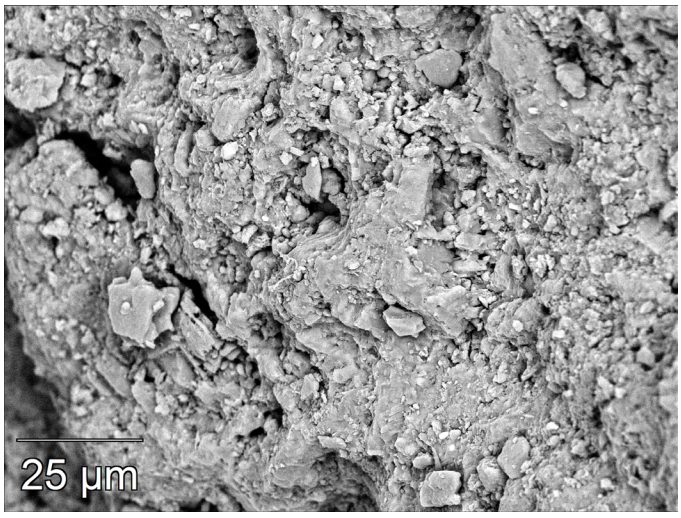

Figure 12. Scanning electron microscope image of sandstone (sample RP-12-7; site 17 on fig. 4) from the upper part of the Proto Canyon member in the Sonoita Creek area showing clinoptilolite in pore space. Note the moderate amounts of open pore space. Clinoptilolite crystals are generally less than 25 micrometers (µm) in size. See figure 11 for photograph of outcrop. Image shows primarily clinoptilolite; smectite and illite clay is likely present, but precise identification of clay could not be determined from these analyses.

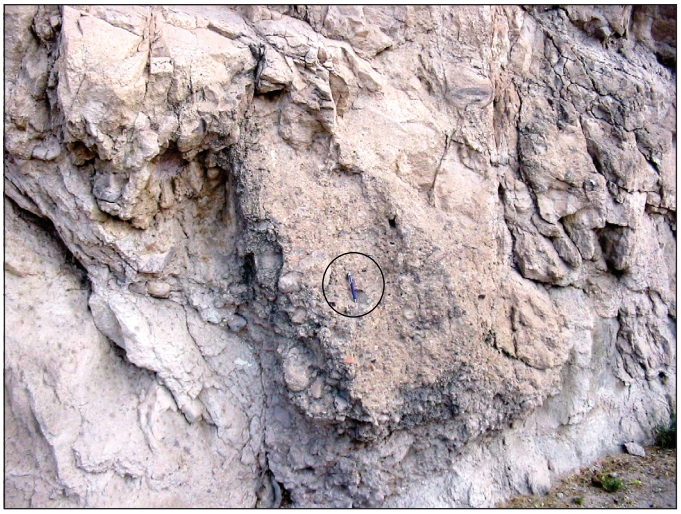

Figure 13. Massive, cliff-forming volcaniclastic sandstone and conglomeratic sandstone in the basal part of the Nogales Wash member in Grand Avenue area, south of Mariposa Road; pen in center for scale. Note the internal deformation, including abundant fractures, and breccia zone in the center of the photograph. Sandstones from the Nogales Wash member are moderately consolidated and brittle, have the highest bulk density in the formation (2.47 grams per cubic centimeter), and are pervasively fractured compared to other members of the formation. Sandstone from this location (sample 10-RP-10; site 9 on fig. 4) has a porosity of 31 percent.

formation (table 2) and corresponds to greater consolidation compared to other members of the formation.

Sample RP-12-46 is from calcareous, conglomeratic sandstone in the middle part of the member (fig. 14). Thin sections show an abundant clay and silt matrix (fig. 15) with some moldic pore space but minimal to no intercrystalline pore space. This rock has a low porosity (22 percent), low bulk density (1.76 gm/cm^3), and intermediate SHC (23.6 cm/d); these findings are consistent with the observation that samples with a mostly silt and clay matrix generally have low porosity and low to intermediate SHC.

The highest SHC in the member (38 cm/d) is from moderately consolidated sandstone in the middle part of the member (sample 10-RP-4; fig. 16) and, like sample 10-RP-10, has abundant fracture porosity and moderate amounts of moldic and intercrystalline pore space. Sample RP-12-15, from the

Figure 14. Conglomeratic sandstone (with mudcracks) in the middle part of the Nogales Wash member; global positioning system (GPS) unit for scale. This rock (sample RP-12-46; site 13 on fig. 4) has a low porosity at 22 percent, a low bulk density at 1.76 grams per cubic centimeter, and an intermediate saturated hydraulic conductivity at 23.6 centimeters per day. Thin sections show an abundant clay and silt matrix with some moldic pore space but minimal to no intercrystalline pore space.

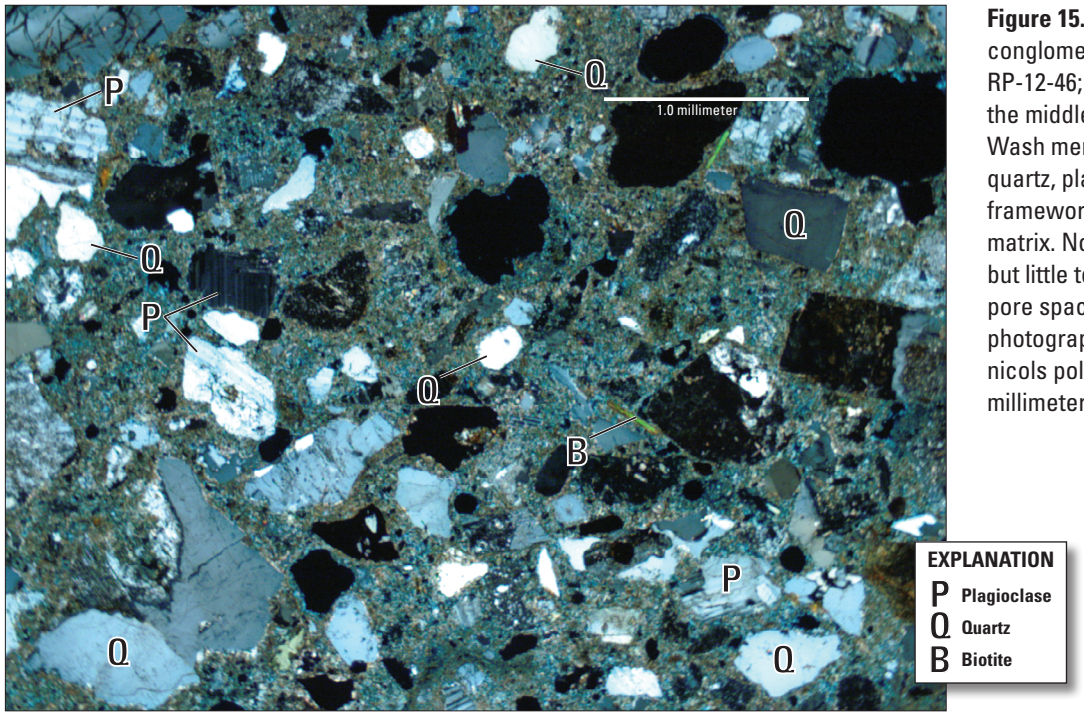

Figure 15. Thin section of conglomeratic sandstone (sample RP-12-46; site 13 on fig. 4) from the middle part of the Nogales Wash member showing mostly quartz, plagioclase, and biotite framework grains in a clay and silt matrix. Note some moldic porosity but little to no intercrystalline pore space. See figure 14 for photograph of outcrop. Cross nicols polarized light. (mm, millimeter)

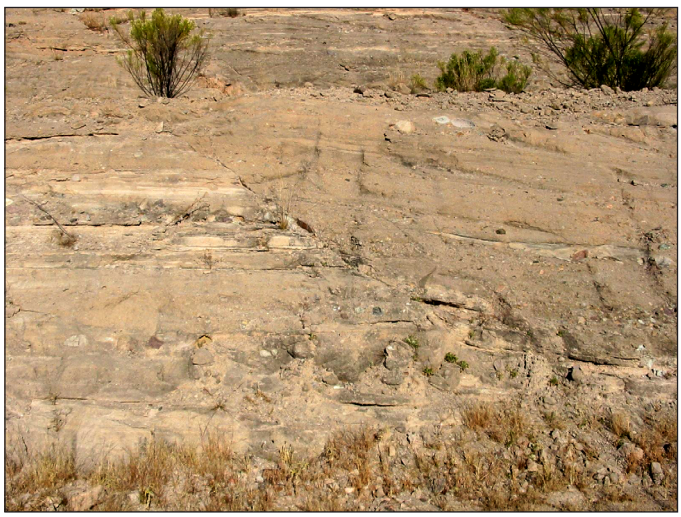

Figure 16. Alternating thin- to thick-bedded sandstone and conglomeratic sandstone of the Nogales Wash member south of Mariposa Road and west of Grand Avenue. A small displacement fault diagonally cuts the beds. Sandstone from this location (sample 10-RP-4; site 8 on fig. 4) has the highest saturated hydraulic conductivity for the member at 38 centimeters per day.

Figure 17. Massive clay unit in the Mariposa member between Interstate 19 and Grand Avenue, south of Mariposa Road. Unit may be a significant local confining unit in the Mariposa member, although its subsurface thickness and lateral extent are poorly known. Note the unit holding water following a rainstorm.

upper part of the member, has an intermediate SHC at 26 cm/d and is from fine-grained, moderately sorted sandstone near the top of the member. Thin sections show a mostly pumice and glass matrix with moderate intercrystalline pore space and minor amounts of moldic pore space.

Sample RP-12-24 is from sandstone near the top of the member at Crawford Hill, along Interstate 19 (fig. 2), which contains mostly pumice, volcanic clasts, and chert. The sample has low porosity (22 percent) and intermediate bulk density (1.86 gm/cm^3). Thin sections show a pumice and glass matrix and abundant moldic and intercrystalline pore space; parts of the matrix are altered to clay.

Mariposa Member

The Mariposa member contains alternating beds of conglomerate, conglomeratic sandstone, siltstone, and claystone. Claystone units are exposed in the lower part of the member in the Mariposa Road area, between Interstate 19 and Grand Avenue (fig. 17). The claystone may be a confining unit within the member, but more subsurface data are needed to determine its subsurface distribution and thickness. The claystone is massive bedded and is estimated to be greater than 60 m (Page and others, 2016). Similar claystone units are exposed in the area east of the Santa Cruz River and south of Sonoita Creek but are generally thinner than the Mariposa Road units.

Four samples of the Mariposa member were analyzed for porosity, and three samples for SHC. Porosity is low to intermediate and ranges from 16 to 36 percent (table 2), and bulk density is low to intermediate and ranges from 1.6 to 2.37 g/cm^3 (table 2). Saturated hydraulic conductivity for the member is also low to intermediate compared to other members and ranges from 5.6 to 33.4 cm/d (table 3).

Both the highest and lowest porosity are from sandstone in the upper part of the member (fig. 2–1*F*), east of the Santa Cruz River and south of Sonoita Creek (figs. 2, 4). Sample RP-12-27 has the highest porosity (36 percent) and highest bulk density at (2.37 g/cm^3) for the member, as well as a moderately high SHC (32.7 cm/d). The sample is from conglomeratic sandstone (fig. 18), and thin sections show abundant moldic and intercrystalline pore space with a matrix of small disaggregated pumice and glass fragments. Scanning electron microscope and x-ray diffraction methods indicate that the sample contains abundant clinoptilolite and lesser smectite, and SEM (fig. 19) shows moderate to abundant amounts of intercrystalline pore space between clinoptilolite crystals, which may explain the moderately high porosity and SHC.

Sample RP-12-11 is also from the upper part of the member and has the lowest porosity of the entire Nogales Formation at 16 percent. It was collected from fine-grained facies of the member, which consist of sequences of sandstone, siltstone, and claystone (fig. 20). Thin sections show a mostly silt and clay matrix (fig. 21), calcite filling some pore space, and minor intercrystalline and moldic porosity. The sample has intermediate bulk density at 2.07 g/cm^3.

Sample 10-RP-2 was collected from a thin sandstone bed in the lower part of the member (fig. 22), in the Mariposa Road area. The sample has low porosity (24 percent), the lowest bulk density (1.6 g/cm^3) for the entire formation, and an intermediate SHC (33.4 cm/d). Thin sections show a mostly

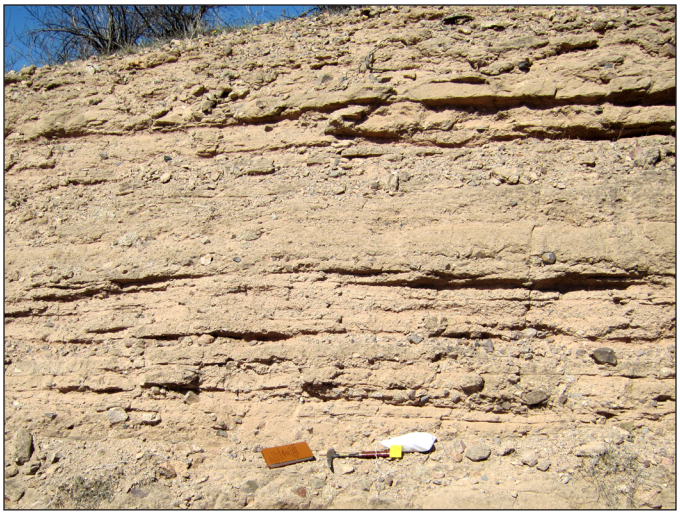

Figure 18. Mariposa member east of the Santa Cruz River and south of Sonoita Creek; hammer and notebook for scale. Sandstone from this location (sample RP-12-27; site 6 on fig. 4) has the highest effective porosity for the member at 36 percent and the highest bulk density for the member at 2.37 grams per cubic centimeter; it has a moderately high saturated hydraulic conductivity at 32.7 centimeters per day.

silt and clay matrix, moderate amounts of intercrystalline pore space, minor fracture porosity, and some large pumice fragments with moderate moldic porosity. X-ray diffraction indicates that the sample contains abundant smectite and minor clinoptilolite.

Sample RP-12-19a from near the base of the member has low porosity (21 percent), moderately high bulk density (2.23 g/cm^3), and the lowest SHC for the member (5.6 cm/d). Thin sections show the rock is moderately sorted and fine grained with a mostly pumice matrix, moderate amounts of moldic porosity within pumice fragments, and minor intercrystalline pore space. Fabric characteristics are similar to the only other moderately sorted, fine-grained sample analyzed (RP-12-7 from the Proto Canyon member), which also has a low porosity at 22 percent.

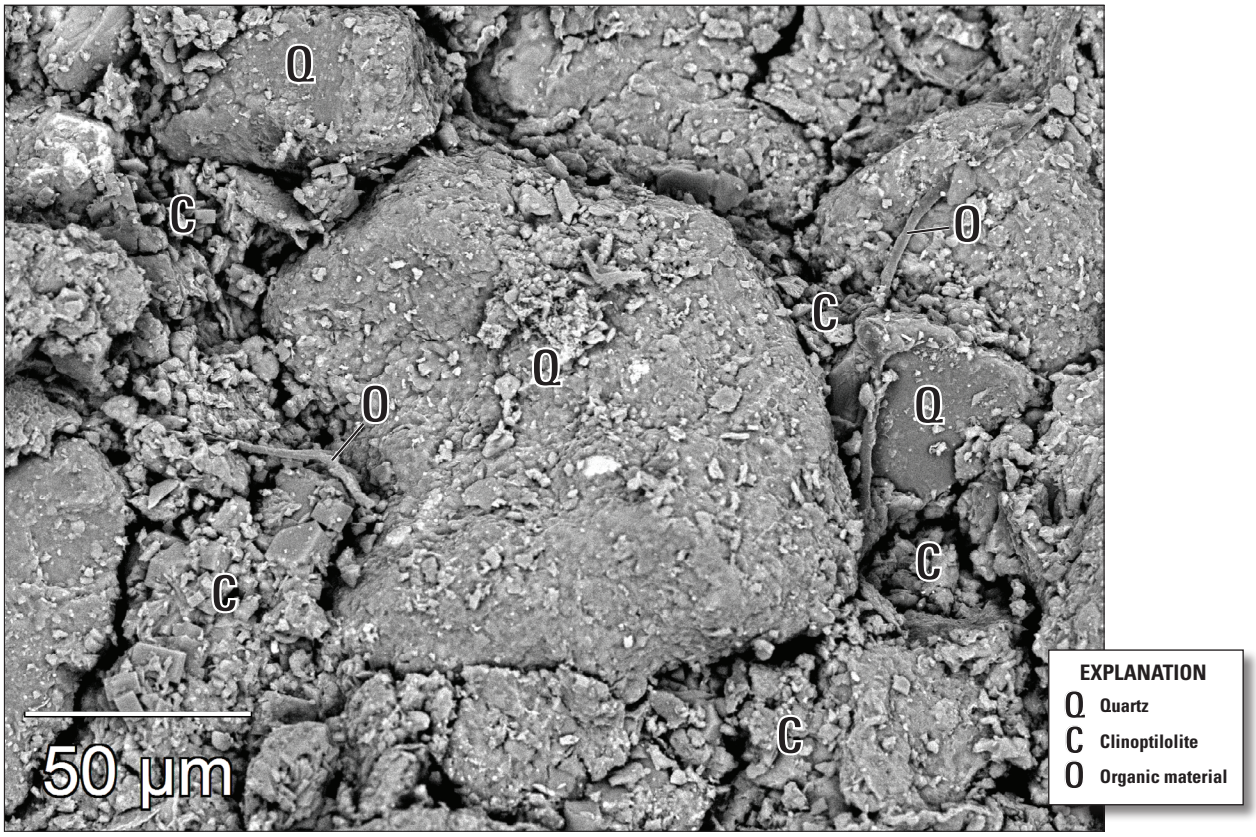

Figure 19. Scanning electron microscope image of sandstone (sample RP-12-27; site 6 on fig. 4) from the Mariposa member. Larger framework grains (mostly quartz) are separated by intercrystalline pore space filled with mostly clinoptilolite crystals and some fibrous organic material. Pore space is generally 50 micrometers (µm) and less in width. See figure 18 for photograph of outcrop.

Figure 20. Fine-grained facies of the Mariposa member, south of Sonoita Creek, east of the Santa Cruz River, and near the Mount Benedict fault, consisting of alternating beds of fine-grained volcaniclastic sandstone, siltstone, and claystone; hammer for scale. Sandstone from this location (sample RP-12-11; site 4 on fig. 4) has the lowest porosity for the entire Nogales Formation at 16 percent. Thin sections (fig. 21) show a mostly silt and clay matrix, calcite filling the pore space, and minor intercrystalline and moldic porosity.

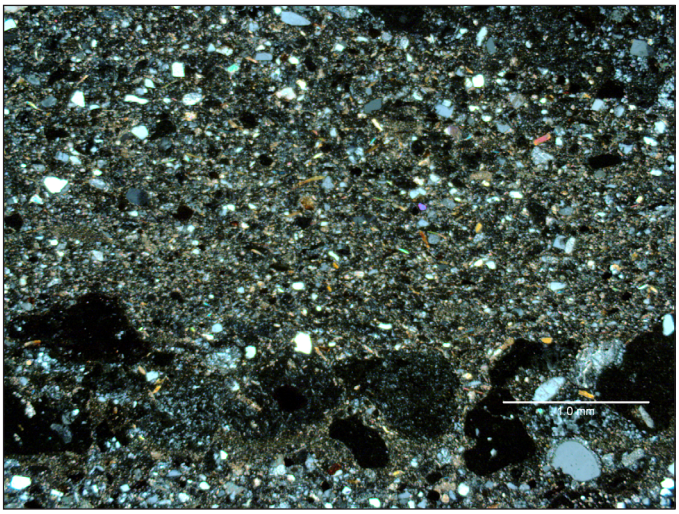

Figure 21. Thin section of sandstone (sample RP-12-11; site 4 on fig. 4) from the Mariposa member, south of Sonoita Creek, east of the Santa Cruz River, and near the Mount Benedict fault, showing a predominantly silt and clay matrix and silt-size grains composed primarily of subangular quartz and minor biotite, hornblende, and plagioclase; several larger, rounded porphyritic volcanic grains are to the left of scale bar. See figure 20 for photograph of outcrop. Cross nicols polarized light. (mm, millimeter)

Figure 22. Thin sandstone bed (7 centimeters thick; outlined by bracket) in Mariposa member. Rock from this bed (sample 10-RP-2; site 1 on fig. 4) has a low porosity at 24 percent, the lowest bulk density for the entire formation at 1.6 grams per cubic centimeter, and an intermediate saturated hydraulic conductivity at 33.4 centimeters per day. The rock has a mostly silt and clay matrix and moderate amounts of intercrystalline and moldic porosity.

Fractures in the Nogales Formation

All members of the Nogales Formation are fractured and faulted from Tertiary Basin and Range extensional deformation, which was contemporaneous with deposition of the formation. Fractures are present in all members of the formation in the Nogales, Ariz., area, but the Nogales Wash member is pervasively fractured compared to the other members. Subvertical, open fractures are present in the Mariposa member, especially in road cuts along Interstate 19 north of Mariposa Road (fig. 23). The Nogales Formation is moderately to highly fractured in other parts of the upper Santa Cruz basin, including the Agua Fria Canyon area (figs. 24) and the Peña Blanca Canyon area (fig. 25), both in the Peña Blanca Lake 7.5' quadrangle (fig. 1). The Nogales Formation in Agua Fria Canyon contains intersecting northwest- and northeast-trending fractures in volcaniclastic sandstone units. Outcrops in the Peña Blanca Canyon area show abundant intersecting fractures in a distinctive, highly brittle ash fall tuff unit in the Nogales Formation.

Fractures in the Nogales Wash and Proto Canyon members are well exposed in several outcrops in the Nogales, Ariz., area, including in urban Nogales, and the Sonoita Creek area; see figure 4 for outcrop locations. We mapped fractures and produced simplified maps of several outcrops using Google Earth imagery (figs. 26, 27), primarily to demonstrate that many parts of the Nogales Formation are fractured in outcrop and that these fracture networks show connectivity in the upper Santa Cruz basin. Although these reconnaissance

Figure 23. Fractures in volcaniclastic sandstone and conglomerate of the Mariposa member north of Mariposa Road and west of Interstate 19.

Figure 24. North-to-northeast view of intersecting fractures (indicated by linear vegetation patterns) in volcaniclasitc sandstone of the Nogales Formation in the Agua Fria Canyon area. Width of view is about 250 meters across.

Figure 25. Aerial view of highly fractured outcrop in ash fall tuff unit in the lower part of the Nogales Formation in the Peña Blanca Lake 7.5′ quadrangle (fig. 1). State Highway 289 is shown near top of image. Top of image is north; width of view is about 175 meters across. (Image from Google, 2014)

studies are mainly for demonstration purposes, comprehensive fracture investigations are needed to better understand and fully evaluate fracture flow in the upper Santa Cruz basin. Future studies should include detailed fracture mapping and description of fracture characteristics important to hydrologic flow modeling, including fracture orientation (azimuth, dip, and dip direction), fracture surface roughness, aperture, trace length, spacing, and connectivity. These types of studies were completed for hydrogeologic modeling in other parts of the Basin and Range Province (for example, Barton and others, 1993), where Tertiary volcanic rocks have also been deformed by episodes of Basin and Range extension.

One prominent outcrop in the Nogales Wash member is northeast of where State Highway 82 joins Grand Avenue (figs. 2, 26); the outcrop contains at least four main fracture sets, including east-northeast (yellow), north-northeast (blue), northeast (green), and northwest (red) trending sets. North-northeast and northeast sets contain the longest through-going fractures. North-northeast fractures are the longest, do not abut other fractures, and cut shorter fractures of the northwest and east-northeast sets. Northeast fractures have long trace lengths, abut fractures in the north-northeast and northwest sets, and intersect northwest fractures. Northwest fractures have some long trace lengths, but they also have shorter fractures which are bound by and break up smaller blocks between longer north-northeast and northeast fractures. The east-northeast set contains the shortest fractures, which also break up blocks between the longer through-going sets.

In the Sonoita Creek area (fig. 27), three fracture sets were mapped in the lower part of the Proto Canyon member: east-northeast (yellow), north-northwest (blue), and

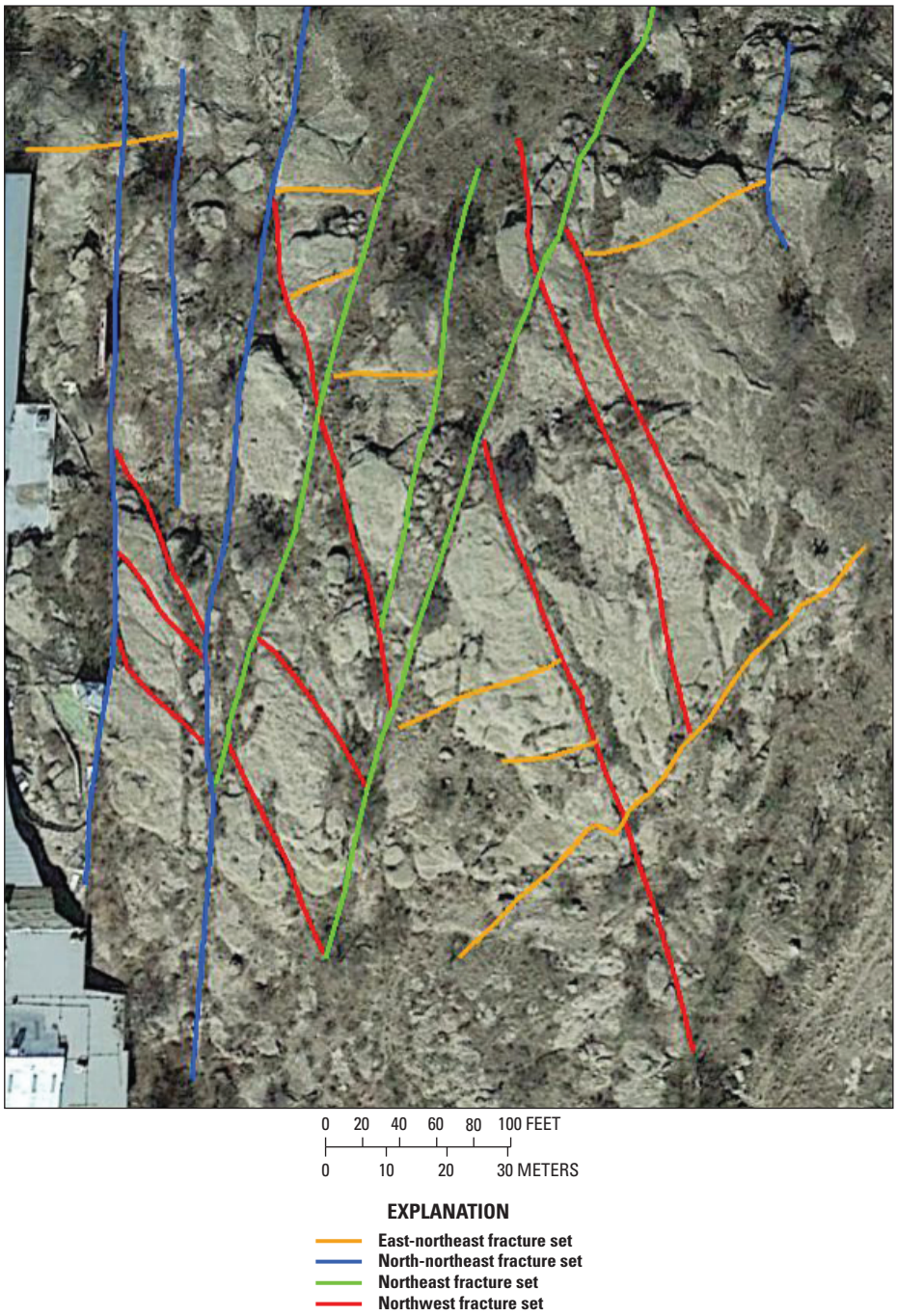

Figure 26. Aerial view of simplified fracture map of the Nogales Wash member of the Nogales Formation northeast of where State Highway 82 joins Grand Avenue. Top of image is north. (Base map from Google, 2015)

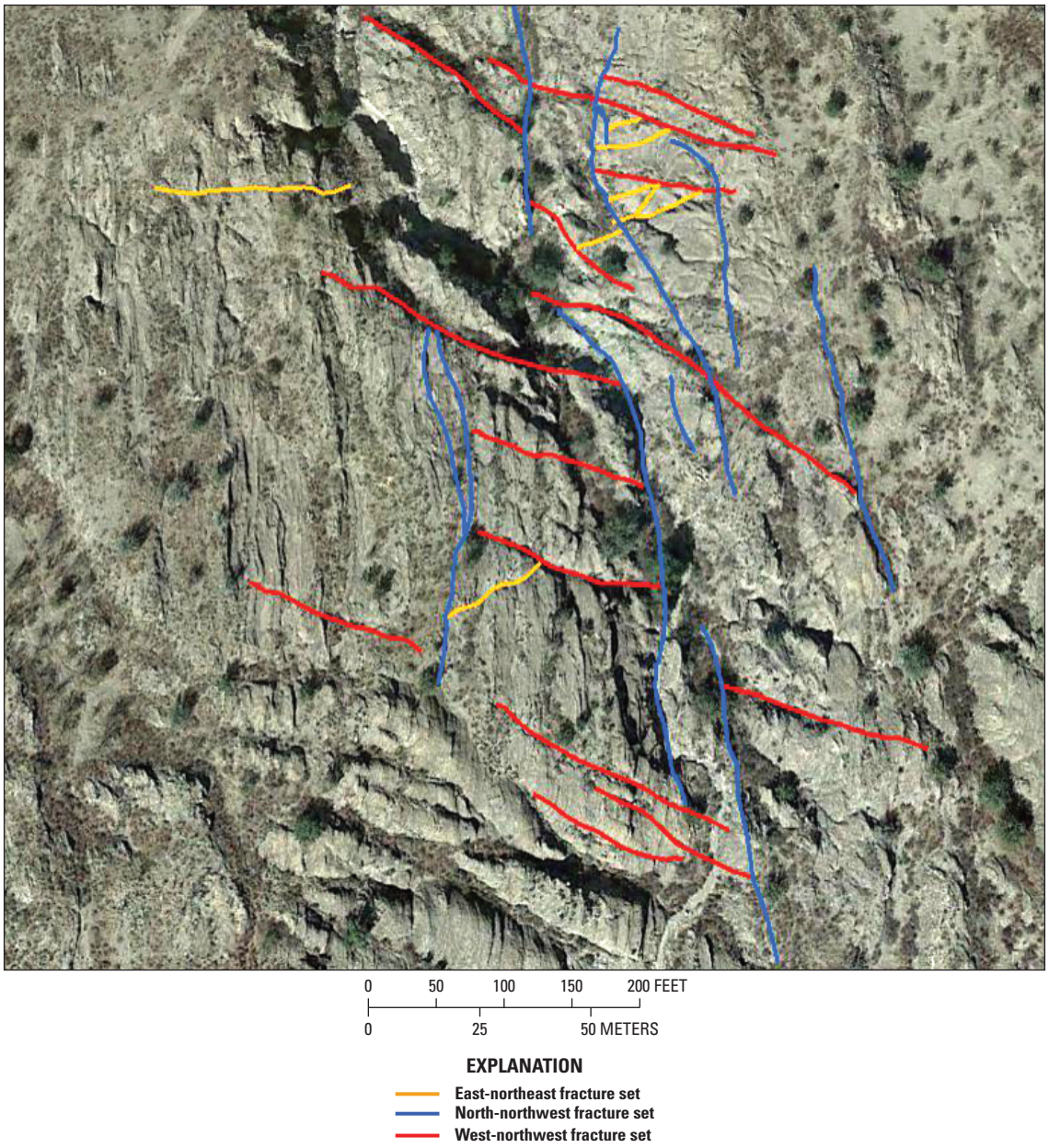

Figure 27. Aerial view of simplified fracture map of the Proto Canyon member of the Nogales Formation in the Sonoita Creek area. West-northwest fractures are the dominant set. Top of image is north. (Base map is from Google, 2015)

west-northwest (red) sets. The north-northwest set contains the longest through-going fractures and intersects fractures of the west-northwest set. The west-northwest set also has some long fractures, but it has shorter fractures which are bound by the longer north-northwest set and break up into smaller blocks between the longer fractures. The east-northeast fractures are similar to those in the Nogales area outcrop and have similar orientations; they generally include smaller fractures which break up blocks between longer through-going fractures.

Summary

New hydrogeologic investigations of the Nogales Formation were conducted to better understand and evaluate the groundwater resource potential of the Nogales Formation in the Nogales, Arizona, area. Preliminary results of these investigations suggest that parts of the Miocene Nogales Formation may be new, deeper sources of groundwater for the area. Our studies are based primarily on detailed geologic mapping and geophysical interpretations of the formation in the Rio Rico and Nogales 7.5' quadrangles (Page and others, 2016).

We analyzed sandstone samples from the formation for porosity, bulk density, saturated hydraulic conductivity (SHC), and fabric. Effective porosity ranges from 16 to 42 percent, bulk density from 1.6 to 2.47 grams per cubic centimeter, and SHC from 4 to 57 centimeters per day. Thin sections indicate a matrix in most samples that consists of disaggregated pumice and volcanic glass fragments; some samples contain predominantly silt and clay. Samples with a mostly silt and clay matrix generally have a lower porosity and SHC compared to samples with a mostly pumice and glass matrix, which generally have a higher porosity and SHC but at much wider ranges.

Most sandstone in the formation is poorly sorted, but several samples are moderately sorted, consist of fine-grained sandstone, and generally have low porosity. Pore space in the Nogales Formation sediments generally included moldic, intercrystalline, and fracture porosity. Some intercrystalline pore space is partially filled with calcite cement. About one third of the samples show fracture porosity, which corresponds to the fracturing noted in outcrops in all members of the formation.

Scanning electron microscope and x-ray diffraction analyses indicate that most of the samples contained the zeolite clinoptilolite and varying amounts of mixed-layer smectite and illite clay. Samples with greater amounts of clinoptilolite and lesser amounts of smectite have high porosity and SHC, in narrow ranges. Samples with abundant amounts of smectite and lesser amounts of clinoptilolite have wide-ranging porosity and SHC, which span the entire ranges of porosity and SHC values reported for the entire formation.

All members of the Nogales Formation are fractured and faulted as a result of Tertiary Basin and Range extensional deformation, which was broadly contemporaneous with deposition of the Nogales Formation. Fractures are present in all members of the formation, but the Nogales Wash member is pervasively fractured compared to the other members. These structures may have significant influence on groundwater flow in the upper Santa Cruz basin.

Acknowledgments

We thank Margaret E. Berry and Harland Goldstein (USGS Geoscience and Environmental Change Science Center, Denver, Colorado) for their reviews; their comments and suggestions vastly improved the report. Gary Skipp (USGS, Denver, Colo.) analyzed samples from the Nogales Formation using x-ray diffraction. Heather Lowers (USGS, Denver, Colo.) prepared samples and assisted the senior author in analyzing samples from the Nogales Formation using the scanning electron microscope. Michelle Stern of the USGS California Water Science Center (USGS Hydrologic Research Laboratory, Sacramento, Calif.) analyzed samples from the Nogales Formation for porosity, saturated hydraulic conductivity, and bulk density. Wagner Petrographic (Lindon, Utah) prepared all thin sections for fabric studies of the Nogales Formation.

References Cited

Barton, C.C., Larsen, Eric, Page, W.R., and Howard, T.M., 1993, Characterizing fractured rock for fluid-flow, geomechanical, and paleostress modeling—Methods and preliminary results from Yucca Mountain, Nevada: U.S. Geological Survey Open-File Report 93–269, 62 p.

Clear Creek Associates, 2011, Hydrogeologic investigations of the Santa Cruz microbasins, Nogales, Arizona: Prepared for the City of Nogales Utilities Department, Arizona, 21 p.

Cosca, M.A., Page, W.R., Gray, Floyd, Lee, J.P., Menges, C.M., and Bultman, Mark, 2013, $^{40}Ar/^{39}Ar$ geochronology of the Oligocene-Miocene Grosvenor Hills volcanics and the Miocene Nogales Formation, upper Santa Cruz basin, southern Arizona [abs.]: Geological Society of America Abstracts with Programs, v. 45, no. 7, p. 129.

Erwin, Gretchen, 2007, Groundwater flow model of the Santa Cruz active management area microbasins, international boundary to Nogales International Wastewater Treatment Plant, Santa Cruz County, Arizona: Arizona Department of Water Resources Modeling Report No. 15, 143 p.

Freeze, R.A., and Cherry, J.A., 1979, Groundwater: Englewood Cliffs, N.J., Prentice Hall, 604 p.

Gettings, M.E., and Houser, B.B., 1997, Basin geology of the upper Santa Cruz valley, Pima and Santa Cruz Counties, southeastern Arizona: U.S. Geological Survey Open-File Report 97–676, 39 p.

Gottardi, Glauco, and Galli, Ermanno, 1985, Natural zeolites: New York, Springer-Verlag, Minerals and Rocks 18, 409 p.

Gray, Floyd, Page, W.R., Bultman, Mark, and Menges, C.M., 2014, Hydrogeologic characteristics of the Miocene Nogales Formation, upper Santa Cruz Basin, southern Arizona [abs.]: Geological Society of America Abstracts with Programs, v. 46, no. 6, p. 118.

Iijima, Azuma, 2001, Zeolites in petroleum and natural gas reservoirs, *in* Bish, D.L., and Ming, D.W., eds., Natural zeolites—Occurrences, properties, and applications: Reviews in Mineralogy and Geochemistry, v. 45, no. 1, p. 347–402.

Menges, C.M., 1981, The Sonoita Creek basin—Implications for late Cenozoic tectonic evolution of basins and ranges in southeastern Arizona: Tucson, University of Arizona, M.S. thesis, 239 p.

Menges, C.M., and McFadden, L.D., 1981, Evidence for a latest Miocene to Pliocene transition from Basin-and-Range tectonic to post tectonic landscape evolution in southeastern Arizona, *in* Stone, Claudia, and Jenny, J.P., eds., Arizona Geological Society digest: Arizona Geological Society Digest XIII, p. 151–160.

Menges, C.M., and Pearthree, P.A., 1989, Late Cenozoic tectonism in Arizona and its impact on regional landscape evolution, *in* Jenny, J.P., and Reynolds, S.J., eds., Arizona Geological Society digest: Arizona Geological Society Digest XVII, p. 649–680.

Nelson, Keith, 2007, Groundwater flow model of the Santa Cruz active management area along the effluent-dominated Santa Cruz River, Santa Cruz and Pima Counties, Arizona: Arizona Department of Water Resources, Modeling Report No. 14, 117 p.

Page, W.R., Menges, C.M., Gray, Floyd, Berry, M.E., Bultman, M.W., Cosca, M.A., and VanSistine, D.P., 2016, Geologic map of the Rio Rico and Nogales 7.5’ quadrangles, Santa Cruz County, Arizona: U.S. Geological Survey Scientific Investigations Map 3354, 32 p. pamphlet, appendix, 2 sheets, scale 1:24,000, http://dx.doi.org/10.3133/sim3354.

Pollastro, R.M., 1982, A recommended procedure for the preparation of oriented clay mineral specimens for X-ray diffraction analysis—Modifications to Drever’s filter-membrane peel technique: U.S. Geological Survey Open-File Report 82–71, 10 p.

Pryor, W.A., 1973, Permeability-porosity patterns and variations in some Holocene sand bodies: American Association of Petroleum Geology Bulletin, v. 57, p. 162–189.

Simons, F.S., 1974, Geologic map and sections of the Nogales and Lochiel quadrangles, Santa Cruz County, Arizona: U.S. Geological Survey Scientific Investigations Map I-762, 9 p. pamphlet, scale 1:48,000.

Sweeney, R.E., and Hill, P.L., 2001, Arizona aeromagnetic and gravity maps and data—A Web site for distribution of data: U.S. Geological Survey Open-File Report 01–0081.

Appendixes

Appendix 1. Thin Section Analyses of the Nogales Formation

Mariposa Member

10-RP-2—Mariposa member, along Mariposa Road between Interstate 19 and Grand Avenue, Nogales, Ariz.; sample site 1; volcaniclastic conglomerate and sandstone, subangular to subrounded, poorly sorted; quartz, plagioclase, microcline, large pumice fragments, biotite, hornblende, small scattered opaques, and some rounded clay; grains highly altered to clay; matrix mostly silt and clay, and some pumice and volcanic glass fragments; moderate moldic and intercrystalline porosity and minor fracture porosity.

10-RP-9—Mariposa member, along Mariposa Road west of Grand Avenue, Nogales, Ariz.; sample site 2; volcaniclastic conglomerate and sandstone, subrounded to subangular, poorly sorted; quartz (larger grains polymictic), highly altered plagioclase, pumice, volcanic glass, hornblende, biotite, chert, and opaques; matrix pumice and volcanic glass fragments, and some silt and clay; moderate intercrystalline, moldic, and fracture porosity; clay replacing highly altered grains and calcite filling some pore space.

RP-12-9—Mariposa member, Sonoita Creek area; sample site 3; volcaniclastic conglomerate and sandstone, bimodal and poorly sorted; large grains subrounded, highly altered hornblende, plagioclase- and biotite-bearing porphyritic volcanic rocks, and some pumice and volcanic glass fragments; smaller grains mostly subrounded and poorly sorted quartz, plagioclase, hornblende, and biotite; matrix mostly grain supported, but some pumice and volcanic glass fragments, silt, and clay; moderate intercrystalline and minor moldic porosity; abundant secondary calcite filling intercrystalline pore space.

RP-12-11—Mariposa member, near exposed Mount Benedict fault; sample site 4; volcaniclastic sandstone, fine- to coarse-grained, subrounded to subangular, poorly sorted; quartz, plagioclase, biotite, and subrounded pumice and volcanic glass fragments, some volcanic porphyritic grains with hornblende and biotite, spherulites, and some opaque grains; contains thin clay layers; matrix mostly silt and clay, and some pumice and volcanic glass; minor moldic and intercrystalline porosity; minor secondary calcite and opaques filling intercrystalline pore space.

RP-12-19a—Mariposa member (base of member), east of Nogales, Ariz., near the international border; sample site 5; volcaniclastic sandstone, fine-grained, subrounded to subangular, moderately sorted; mostly pumice and volcanic glass fragments with lesser quartz, plagioclase, hornblende, biotite, chert, and scattered opaques; matrix pumice and volcanic glass fragments, and grain supported where matrix absent; moderate moldic and minor intercrystalline porosity.

RP-12-27—Mariposa member, south end of exposed Mount Benedict fault; sample site 6; volcaniclastic sandstone, subrounded to subangular, poorly sorted; quartz, plagioclase, pumice, volcanic glass, biotite, hornblende, volcanic porphyritic grains with biotite and hornblende, opaques, and chert; matrix pumice and volcanic glass fragments; abundant moldic and intercrystalline porosity; minor calcite in pore space; clay replacing highly altered plagioclase and pumice grains.

RP-12-29—Mariposa member, fine-grained facies south of Sonoita Creek and east of Santa Cruz River; sample site 7; volcaniclastic sandy claystone to clayey sandstone and conglomerate, subrounded to subangular, poorly sorted; quartz, highly altered plagioclase, biotite, pumice, volcanic glass, porphyritic volcanic grains with highly altered biotite, and opaques; matrix mostly iron-stained silt and clay, and some pumice and glass fragments; abundant fracture, intercrystalline, and moldic porosity; calcite cement filling intercrystalline pore space.

Nogales Wash Member

10-RP-4—Nogales Wash member, west side of Grand Avenue south of Mariposa Road, Nogales, Ariz.; sample site 8; volcaniclastic sandstone, subangular to subrounded, poorly sorted; pumice and volcanic glass fragments, quartz, plagioclase, biotite, hornblende, spherulites, large volcanic porphyritic grains with plagioclase, biotite, and hornblende; matrix pumice and volcanic glass fragments; abundant fracture porosity, moderate intercrystalline and moldic porosity.

10-RP-10—Nogales Wash member, Grand Avenue area south of Mariposa Road, Nogales, Ariz.; sample site 9; volcaniclastic sandstone and conglomerate, subangular to subrounded, poorly sorted; pumice and volcanic glass fragments, quartz, lesser plagioclase, small volcanic porphyritic grains with plagioclase laths, biotite, hornblende, opaques, microcline, and chert; matrix mostly pumice and volcanic glass fragments, with some silt and clay; abundant fracture porosity, moderate moldic and intercrystalline porosity.

RP-12-15—Nogales Wash member, near the international border; sample site 10; volcaniclastic sandstone, fine-grained, subangular to subrounded, moderately sorted; pumice and volcanic glass fragments, equal amounts of smaller crystals of subangular quartz and plagioclase, biotite, hornblende, chert, volcanic porphyritic grains with plagioclase laths, and some opaque grains in pore space; matrix pumice and volcanic glass fragments, and grain-supported where matrix absent; moderate intercrystalline and minor moldic porosity.

RP-12-16—Nogales Wash member (lower to basal part of member), east of Nogales, Ariz., near the international border; sample site 11; volcaniclastic sandstone, fine-grained, subangular to subrounded, moderately sorted; pumice and volcanic glass, equal amounts of quartz and plagioclase, biotite, microcline, hornblende, scattered opaques, and some opaques replacing biotite; matrix pumice and volcanic glass fragments, and some grain-supported layers with minor hematite where matrix is absent; moderate moldic and intercrystalline porosity.

RP-12-24—Nogales Wash member, Crawford Hill road cut; sample site 12; volcaniclastic sandstone and conglomerate, subrounded to subangular, very poorly sorted; volcanic porphyritic grains with plagioclase and hornblende, quartz, plagioclase, hornblende, sanidine, pumice and volcanic glass, rounded chert, spherulites, and some opaques; matrix mostly pumice and volcanic glass fragments; abundant moldic and intercrystalline porosity.

RP-12-46—Nogales Wash member, City Hall, Grand Avenue, Nogales, Ariz.; sample site 13; conglomeratic sandstone, subangular to subrounded, very poorly sorted; quartz, plagioclase, bitotite, large rounded iron-stained quartzose sandstone clasts, and granitic porphyritic clasts; matrix mostly clay and silt; minor moldic porosity and minimal to no intercrystalline pore space.

Proto Canyon Member

10-RP-3—Proto Canyon member, north of Mariposa Road between Grand Avenue and Interstate 19, Nogales, Ariz.; sample site 14; volcaniclastic sandstone, subangular to subrounded, poorly sorted; mostly quartz (some larger grains polymictic), plagioclase, lesser microcline, biotite, hornblende, volcanic porphyritic grains with biotite, pumice, and opaques; matrix pumice and volcanic glass fragments; moderate to abundant fracture, intercrystalline, and moldic porosity.

RP-12-4a—Proto Canyon member, east side of Grande Avenue north of Mariposa Road, Nogales, Ariz.; sample site 15; volcaniclastic sandstone and conglomerate, subangular to subrounded, poorly sorted; coarse polymitic strained quartz and plagioclase (undulose extinction), biotite, hornblende, pumice and volcanic glass fragments, and volcanic porphyritic grains with biotite, hornblende, and some plagioclase; matrix mostly silt and clay, with some pumice and volcanic glass; abundant fracture porosity, minor intercrystalline and moldic porosity; moderate to abundant calcite filling intercrystalline pore space, clay replacing large corroded grains of quartz and plagioclase.

RP-12-7—Proto Canyon member, Sonoita Creek area; sample site 17; volcaniclastic sandstone, fine-grained, mostly subrounded, moderately sorted; pumice and volcanic glass fragments, volcanic porphyritic grains with biotite and quartz, lesser quartz, plagioclase, biotite, hornblende, and microcline; matrix pumice and volcanic glass fragments; moderate moldic and moderate to abundant micro-intercrystalline porosity between small, disaggregated pumice fragments.

RP-12-8—Proto Canyon member, Sonoita Creek area; sample site 18; volcaniclastic conglomerate and sandstone, poorly sorted; mostly pumice and large volcanic porphyritic grains with highly altered plagioclase, lesser subangular quartz, plagioclase, hornblende, biotite, opaques, and chert; matrix mostly pumice and volcanic glass fragments; moderate moldic and minor intercrystalline porosity.

RP-12-14—Proto Canyon member, east of Nogales, Ariz., along the international border; sample site 19; volcaniclastic sandstone and pebble conglomerate, subangular, poorly sorted; mostly pumice and volcanic glass, equal amounts of highly altered quartz and plagioclase, biotite, hornblende, and volcanic porphyritic grains with plagioclase laths; matrix silt, clay, and pumice; moderate moldic and minor intercrystalline porosity.

RP-12-21—Proto Canyon member, Proto Canyon; sample site 20; volcaniclastic sandstone and conglomerate, subangular, poorly sorted; large pumice fragments, subangular quartz, biotite, plagioclase, hornblende, chert, and claystone; matrix mostly pumice and volcanic glass fragments; moderate moldic and minor intercrystalline porosity.

RP-12-32—Proto Canyon member, Proto Canyon area; sample site 21; volcaniclastic sandstone, subangular to subrounded, poorly sorted; quartz, plagioclase, pumice, hornblende, biotite, opaques, porphyritic volcanic fragments, and chert; matrix combination of silt, clay and pumice; includes silt and clay layers; moderate moldic and minor intercrystalline porosity.

RP-12-42a—Proto Canyon member, Yerba Buena Canyon; sample site 22; volcaniclastic sandstone, subangular to subrounded, poorly sorted; pumice, quartz, plagioclase (highly altered to clay), porphyritic volcanic fragments, biotite, hornblende, chert, quartzose sandstone fragments, and opaques; matrix combination of pumice, silt, and clay; moderate moldic and minor intercrystalline porosity.

Appendix 2. Values of Bulk Density, Effective Porosity, and Saturated Hydraulic Conductivity For the Nogales Formation

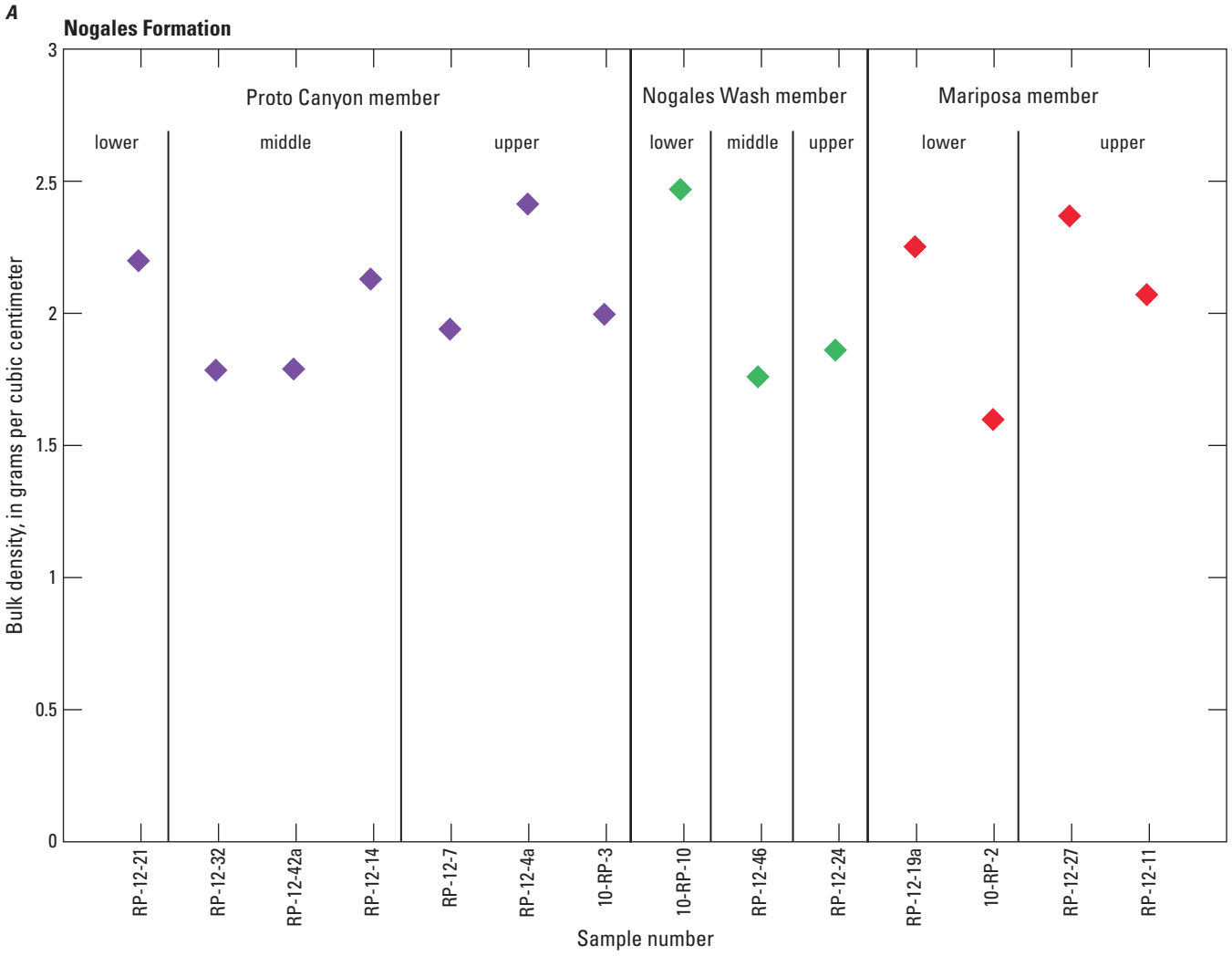

Figure 2–1. Plots of bulk density, effective porosity, and saturated hydraulic conductivity (SHC) for the Nogales Formation, by member. *A*, Bulk density for all members of the Nogales Formation. *B*, Effective porosity for the Proto Canyon member. *C*, SHC for the Proto Canyon member. *D*, Effective porosity for the Nogales Wash member. *E*, SHC for the Nogales Wash member. *F*, Effective porosity for the Mariposa member. *G*, SHC for the Mariposa member.

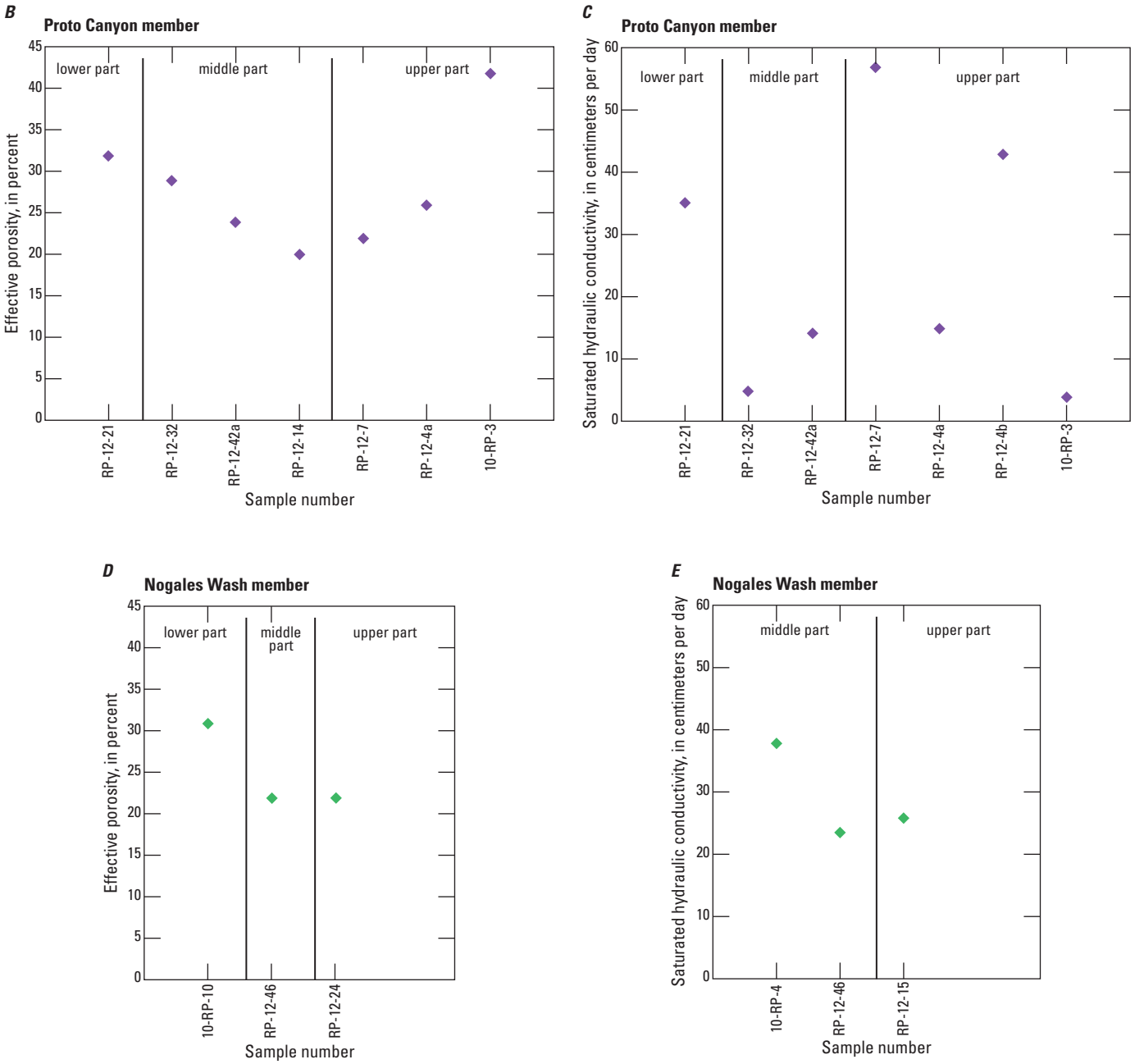

Figure 2–1.—Continued Plots of bulk density, effective porosity, and saturated hydraulic conductivity (SHC) for the Nogales Formation, by member. *A*, Bulk density for all members of the Nogales Formation. *B*, Effective porosity for the Proto Canyon member. *C*, SHC for the Proto Canyon member. *D*, Effective porosity for the Nogales Wash member. *E*, SHC for the Nogales Wash member. *F*, Effective porosity for the Mariposa member. *G*, SHC for the Mariposa member.

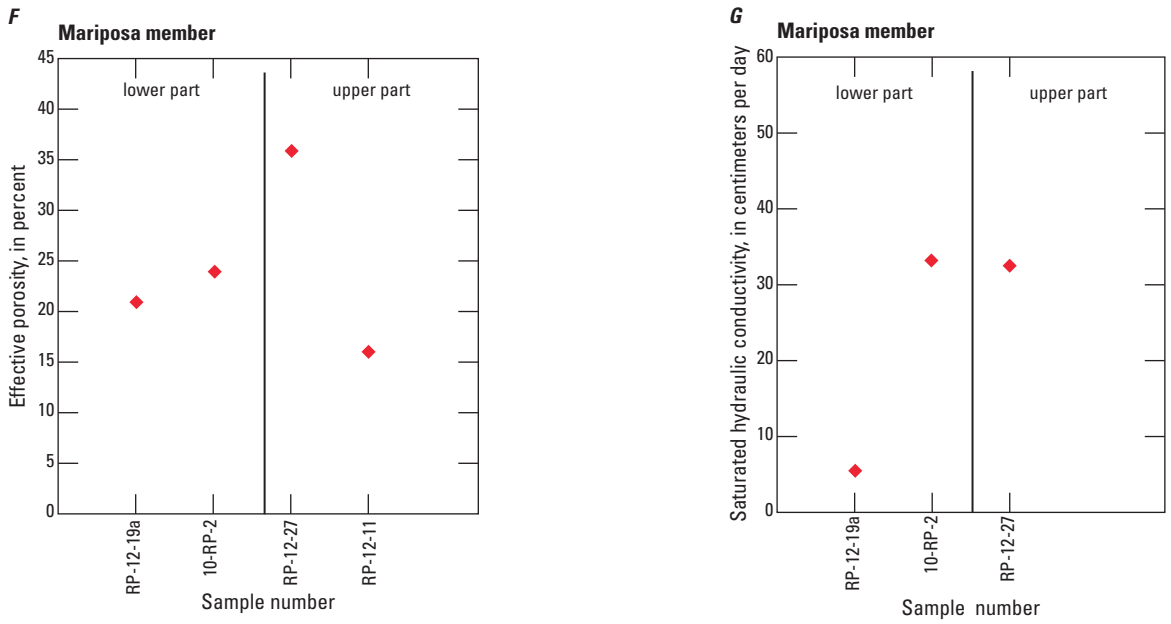

Figure 2–1.—Continued Plots of bulk density, effective porosity, and saturated hydraulic conductivity (SHC) for the Nogales Formation, by member. *A*, Bulk density for all members of the Nogales Formation. *B*, Effective porosity for the Proto Canyon member. *C*, SHC for the Proto Canyon member. *D*, Effective porosity for the Nogales Wash member. *E*, SHC for the Nogales Wash member. *F*, Effective porosity for the Mariposa member. *G*, SHC for the Mariposa member.

Appendix 3. Porosity, Saturated Hydraulic Conductivity, and Bulk Density Analyses and Scanning Electron Microscope and X-Ray Diffraction Methods

Porosity, Bulk Density, and Saturated Hydraulic Conductivity

Samples for porosity, bulk density, and saturated hydraulic conductivity (SHC) were analyzed by the U.S. Geological Survey (USGS) Hydrologic Research Laboratory (HRL) in Sacramento, California. For a detailed summary of the physical properties methods used, see USGS Technical Procedure USGS-HP-229, R3. Determinations of gravimetric and volumetric water content and of bulk density, porosity, and particle density were obtained using a saturation chamber and a laboratory drying oven and were calibrated using balances and Archimedes methods.

Effective porosity (in percent) was calculated by the equation

$$\text{Effective porosity} = \text{Porosity} - \text{Residual water content}$$

where

$$\text{Residual water content} = \frac{\text{Relative humidity dry weight (g)} - \text{Oven dry weight (g)}}{\text{Sample bulk volume}}.$$

The relative humidity dry weight (in grams) was measured at 60 °C and 65 percent humidity. Bulk density (in grams per cubic centimeter) was calculated as dry weight over sample bulk volume. Data on SHC were collected from the Tri-flex 2 Permeameter in accordance with the American Society for Testing and Materials Procedure D5084; conductivities were corrected to 20 °C. All measurement devices were calibrated to National Institute of Standards and Technology traceable standards, and a documented quality assurance program at the USGS HRL ensured minimal error in the measurements.

Scanning Electron Microscope

For scanning electron microscope (SEM) analyses, rock chips were mounted on carbon tape adhered to an aluminum sample stub and coated with carbon for conductivity. The rock chips were placed in a JEOL 5800LV scanning electron microscope operated at 15 kilovolts and a 1-nanoampere current at high vacuum. The chips were examined in both secondary and backscattered electron imaging modes. Qualitative chemistry was acquired from spots of interest with a Thermo Fisher silicon drift detector and USGS National Streamflow Statistics software (http://water.usgs.gov/software/NSS/).

X-Ray Diffraction

For x-ray diffraction (XRD) analyses, clay separation and preparation included removing a representative split of each sample, which was disaggregated and placed in a beaker with distilled water and placed in an ultrasonic for 4–6 minutes. Suspended material was decanted into 250-milliliter centrifuge bottles and centrifuged at the appropriate speed and time for a <2-micrometer size separation. The clay size separation was then mounted on a glass slide according to the preparation of Pollastro (1982) using the Millipore filter transfer method. Clay mounts were analyzed after they were air-dried, glycolated, and heated to 550 °C. The XRD analyses were performed on a Philips 3600 diffractometer using copper radiation. Operating conditions were 30 milliamperes and 40 kilovolts. X-ray diffraction data were collected at 0.02° 2 Θ steps using a 2-second dwell per step. Oriented clay mounts were scanned from 2 to 35° 2 Θ.

Publishing support provided by:
Denver Publishing Service Center

For more information concerning this publication, contact:
Center Director, USGS Geosciences and Environmental Change Science Center
Box 25046, Mail Stop 980
Denver, CO 80225
(303) 236-5344

Or visit the Geosciences and Environmental Change Science Center Web site at:
http://gec.cr.usgs.gov/

USGS

Page and others—**Hydrogeologic Investigations of the Miocene Nogales Formation, Nogales Area, Upper Santa Cruz Basin, Arizona**—SIR 2016–5087

ISSN 2328-0328 (online)
http://dx.doi.org/10.3133/sir20165087